Available online at www.sciencedirect.com

SCIENCE DIRECT®

Tectonophysics 396 (2005) 1–34

TECTONOPHYSICS

www.elsevier.com/locate/tecto

Revision of the timing, magnitude and distribution of Neogene rotations in the western Aegean region

D.J.J. van Hinsbergen[a,*], C.G. Langereis[a,b], J.E. Meulenkamp[a]

[a]*Vening Meinesz Research School of Geodynamics (VMSG), Utrecht University, Faculty of Geosciences, Budapestlaan 4, 3584 CD Utrecht, The Netherlands*

[b]*Paleomagnetic Laboratory 'Fort Hoofddijk', Budapestlaan 17, 3584 CD Utrecht, The Netherlands*

Received 10 March 2004; accepted 15 October 2004
Available online 8 December 2004

Abstract

To evaluate the dimension and the timing of the clockwise rotating domain and the nature of the structures that accommodate the rotating domain in the western Aegean region, paleomagnetic analyses were carried out in northern, western and southwestern Greece. The results show that the rotating domain covers an area including the external Albanides, western mainland Greece including Evia and probably at least partly the Peloponnesos. Smaller clockwise rotations on the order of 30–40° were reported previously from the Chalkidiki peninsula and the islands of Skyros and Limnos. Previously, two phases of approximately 25° of rotation were suggested, the last one during the Plio-Pleistocene. Our analysis shows that the western Aegean domain rotated approximately 40° clockwise between 15–13 and 8 Ma, followed by an additional 10° after 4 Ma.

The rotating domain is accommodated in the north by deformation associated with the Scutari–Pec fault zone and in the west by the Ionian thrust and the Hellenic subduction zone. To the south, no rocks older than ~10 Ma are available so no conclusive data are obtained. To the east of the rotating domain, extensional detachment systems of the Cyclades and Rhodope areas were active during the rotation phase and may explain at least part of the differences in finite amounts of rotation between nonrotation or counterclockwise rotations observed in northern and eastern Greece and the large clockwise rotations in western Greece.

Keywords: Paleomagnetism; Greece; Tectonics; Basins; Deformation; Mediterranean

1. Introduction

The Aegean region has been subjected to extension since the Oligocene (Gautier et al., 1999; Jolivet et al., 2003; Jolivet and Patriat, 1999). This resulted in the formation of metamorphic core complexes, especially during the Miocene, and the foundering of a series of

* Corresponding author. Present address: Department of Geology, University of Leicester, University Road, Leicester LE1 7RH, UK. Tel.: +44 116 2523629.

E-mail address: dvh1@le.ac.uk (D.J.J. van Hinsbergen).

0040-1951/$ - see front matter
doi:10.1016/j.tecto.2004.10.001

Mio-Pleistocene extensional basins in the central and southern Aegean (Angelier, 1981; Gautier et al., 1999; Le Pichon and Angelier, 1979; McKenzie, 1978; Meulenkamp et al., 1988; Fig. 1). At least part of the extensional history of the Aegean is associated with rotations on various scales. Extensive research has been carried out on the rotational history of the Aegean region (e.g., Duermeijer et al., 2000; Horner and Freeman, 1983; Kissel et al., 2003; Kondopoulou, 2000; Laj et al., 1982; Mauritsch et al., 1995; Speranza et al., 1995), indicating large clockwise rotations in western Greece and Albania. Kissel and Laj (1988), Speranza et al. (1995) and Kissel et al. (2003) suggested that clockwise rotation occurred in western Greece in two phases of approximately 25° each, one during the middle to late Miocene and one during the Plio-Pleistocene. Walcott and White (1998) attempted to identify the structures that accommodate the rotational motion based on analysis of stretching lineations in the ductile deformed basement of the

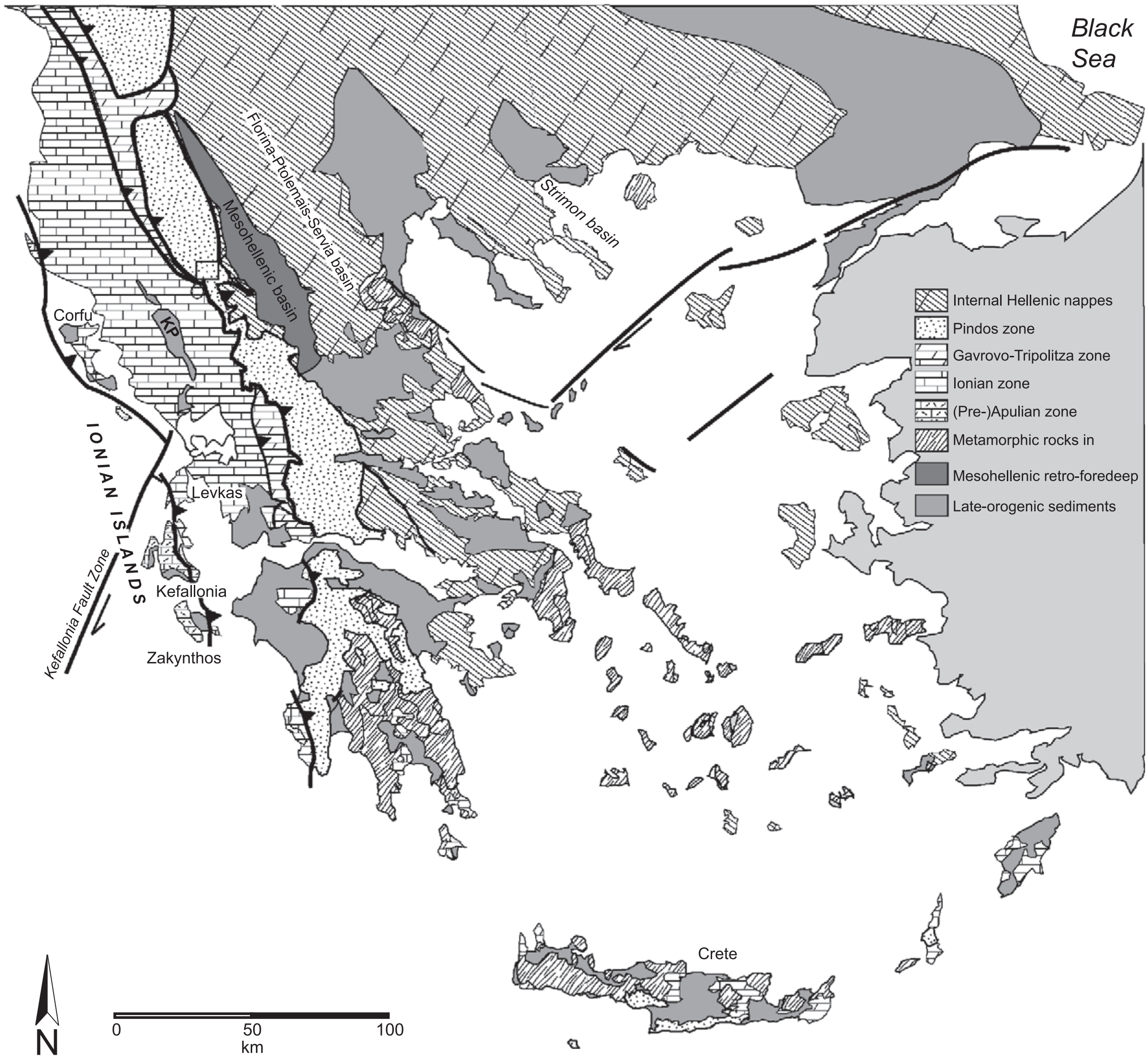

Fig. 1. Tectonic map of Greece, modified after Bornovas and Rontogianni-Tsiabaou (1983) and Jolivet et al. (in press). KP=Klematia–Paramythia basin (Botsara syncline).

internal Hellenides. Their results were in agreement with a ~50° clockwise rotation of western Greece.

To further constrain the relation between rotation and deformation, we analysed and evaluated the timing and magnitude of the rotations of western Greece, and the dimensions of the rotating domains. To this end, we carried out paleomagnetic analyses in northern and western Greece, the Ionian islands, the Peloponnesos, and the islands of Aegina and Kythira, to reevaluate previous work and to include new areas of which no or few rotation data were published. The latter include the Florina–Ptolemais–Servia Basin and the Mesohellenic Basin in northern Greece (Fig. 1). The combination of these new data and published information allows us to reconstruct the relationship between central Aegean extension, rotation and external Aegean compression.

2. Sections, sites and sampling

A total of 2374 cores from 34 localities of Tertiary sedimentary rocks from northern and western Greece, the Peloponnesos, and the islands of Corfu, Kefallonia, Aegina and Kythira were sampled and analysed. A locality was defined as a coherent geological area (e.g., an anticline, an island or a sedimentary section) and contains 1 to 13 sites or sections, each with at least eight samples.

2.1. Strimon Basin (northern Greece)

The Strimon basin in northern Greece is filled with Upper Miocene and Plio-Pleistocene terrestrial and marine sediments. It underwent Late Miocene and Pliocene extension and subsidence, possibly associated with strike–slip movements in the North Aegean Trough along a splay of the North Anatolian Fault Zone (Dinter and Royden, 1993; Dinter, 1998; Snel et al., in press). This younger extensional deformation was superimposed on older extension that created the NW–SE striking, SW verging Strimon–Thassos extensional detachment, along which the Rhodope metamorphic core complex was exhumed during the Early to Late Miocene (Dinter, 1998; Lips et al., 2000; Ricou et al., 1998).

The basin fill consists of a series of fluvio-lacustrine conglomerates and finer sediments, followed by alternating clastics and carbonates, deposited in lacustrine, brackish water or shallow marine depositional environments. During the Late Miocene (Messinian), marine clays were deposited with gypsum lenses, followed by terrestrial sedimentation (Meulenkamp, 1979; Steffens et al., 1979). Our study includes data from the magnetostratigraphic study of Snel et al. (in press) for evaluating rotations in the Strimon Basin.

2.2. Florina–Ptolemais–Servia Basin (northwestern Greece)

West of the Strimon Basin, a series of Late Miocene to Early Pliocene intramontane lacustrine basin sediments overlie rocks of the (Sub-) Pelagonian Zone (Fig. 2). These basins developed in response to NE–SW extension (Caputo and Pavlides, 1993; Pavlides et al., 1998; Pavlides and Mountrakis, 1987) and their stratigraphy was extensively studied by Van Vugt (2000) and Steenbrink (2001). The basin fill is dominated by alternating lacustrine lignite and carbonate beds. These are accurately dated by a combination of magneto-, bio- and cyclostratigraphy and range in age from 8 to 4 Ma (Van Vugt et al., 1998; Steenbrink et al., 1999, 2000; Steenbrink, 2001). We interpreted the samples from seven (composite-) sections (697 cores) that were previously sampled and analysed for magnetostratigraphy by these authors.

2.3. Mesohellenic Basin (northwestern Greece)

The geologic history of the Mesohellenic Basin was described by, e.g., Zygojannis and Müller (1982), Barbieri (1992a,b), Doutsos et al. (1994), Zelilidis and Kontopoulos (1997), Kontopoulos et al. (1999), Avramidis et al. (2002) and Zelilidis et al. (2002). It is a 130-km-long and 40-km-wide, NW–SE striking asymmetric basin, located on top of the (Sub-) Pelagonian and Pindos zones. It is bounded in the west by the east-verging Krania and Eptachori thrusts (Fig. 2) that controlled the Eo-Oligocene sedimentary history of the basin. In the east, the deposits of the Mesohellenic Basin generally onlap on the rocks of the (Sub-) Pelagonian Zone. Seismic data indicate a stratigraphic thickness of up to 4500 m (Kontopoulos et al., 1999). The oldest sediments

Fig. 2. Geologic map of northwestern Greece, modified after Bornovas and Rontogianni-Tsiabaou (1983) with sample locations and measured declination directions.

in the Mesohellenic Basin are found near Krania, southeast of Grevena (Zelilidis et al., 1997; Zygojannis and Müller, 1982; Fig. 2). Conglomerate deposition was followed by Eocene clays with interbedded turbiditic sandstones in an open-marine environment. Further north near Eptachorion, the basal stratigraphy of the Mesohellenic Basin has a younger age (early Oligocene) and displays a sequence of conglomerates, overlain by a series of clay and marls interpreted as shelf-sediments, followed by a submarine fan system characterised by turbiditic sandstones (Avramidis et al., 2002; Barbieri, 1992b; Zygojannis and Müller, 1982).

We sampled 23 sites (223 cores) of marine sediments of the Mesohellenic Basin (Fig. 2). Locality EE consists of 13 sites: 7 sites in the shelf sediments near Eptachorion and 6 sites in the fine parts between the submarine fan-associated turbiditic sandstones along the section EE′ of Avramidis et al. (2002) containing Eocene–Middle Miocene sediments. Likewise, locality DD consists of 7 sites in the basal, Eocene clays near Krania and 2 sites were sampled along the transect DD′ of Avramidis et al. (2002) containing Eocene–Middle Miocene sediments. Additionally, 10 cores were collected from one site in the lower Pliocene shallow marine marls north of Klimataki (locality KH) described by Fountoulis et al. (2001).

2.4. Epirus, Corfu, Akarnania and Kefallonia (western Greece)

In western Greece, Mesozoic to Paleogene sedimentary rocks of the Tripolitza and Ionian Zone nappes are exposed (Fig. 3; e.g., Avramidis et al., 2000; B.P. Co. Ltd., 1971; IGRS-IFP, 1966; Underhill, 1988, 1989): The Tripolitza Zone underthrusted

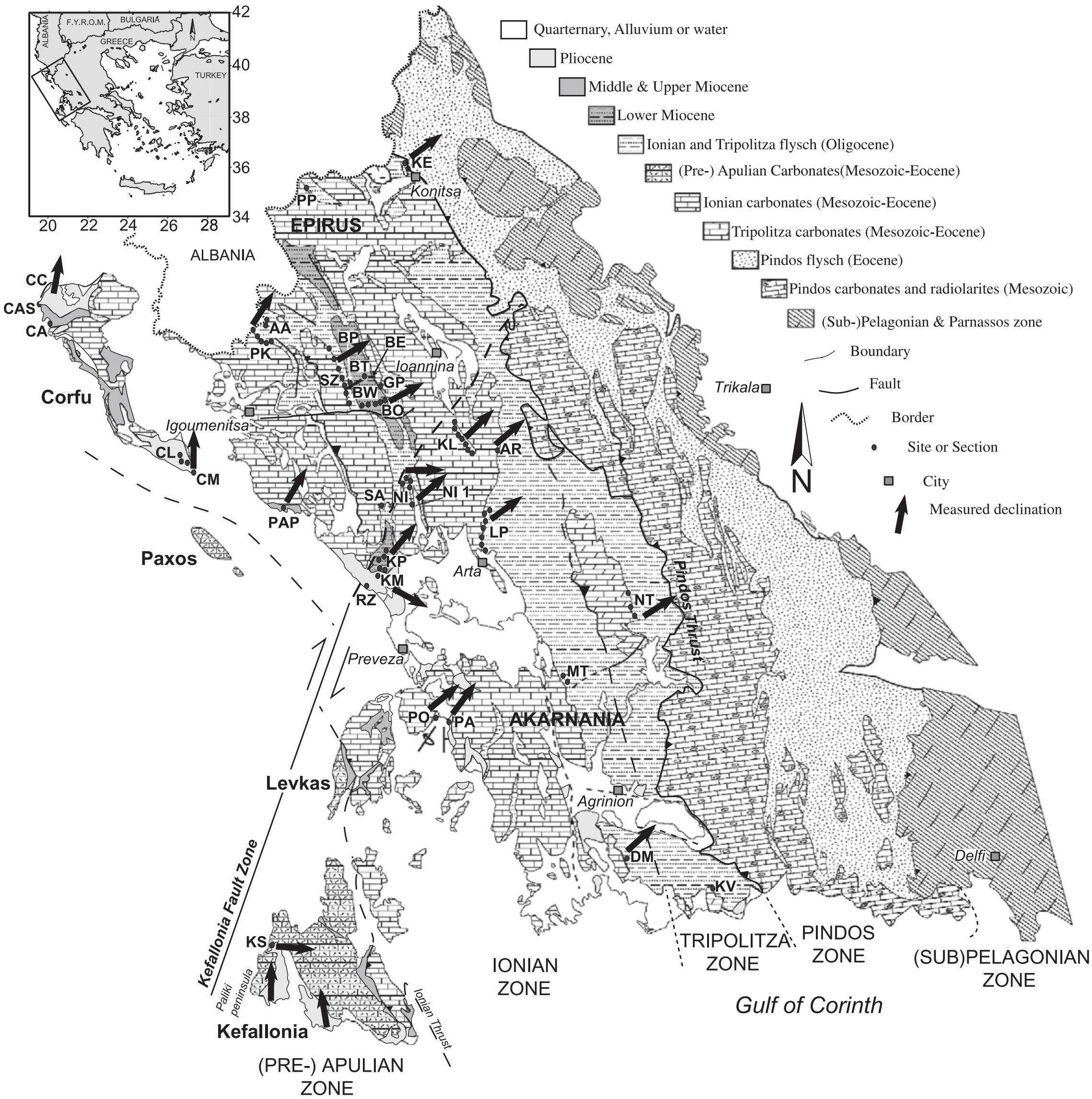

Fig. 3. Geologic map of western Greece, modified after Bornovas and Rontogianni-Tsiabaou (1983) with sample locations and measured declination directions.

the Pindos zone and structurally overlies the Ionian zone, which itself is deformed by several folds and thrusts (Fig. 3). On the Ionian islands of Levkas, Kefallonia and Zakynthos and on the Karaburun peninsula in southern Albania, the Ionian zone overthrusts the (Pre-) Apulian Zone (Cushing, 1985; Meco and Aliaj, 2000; Mercier et al., 1972, 1976; Sorel et al., 1976; Underhill, 1988, 1989).

The nappe stack is crosscut by a number of transverse structures: ENE–WSW trending north-verging half-grabens. The bounding faults of these are still seismically active (e.g., Gulf of Patras–Gulf of Corinth graben, Lake Trichonis and the Amvrakikos–Sperchios grabens: Clews, 1989; Doutsos et al., 1988, 1990; Mariolakos, 1976; Sorel, 2000). Additionally, offshore western Greece, the seismically highly active dextral Kefallonia Fault Zone presently delimits the active outward motion of the Hellenides (Billiris et al., 1991; Cocard et al., 1999; Kahle et al., 1998; Peter et al., 1998). Onshore, a

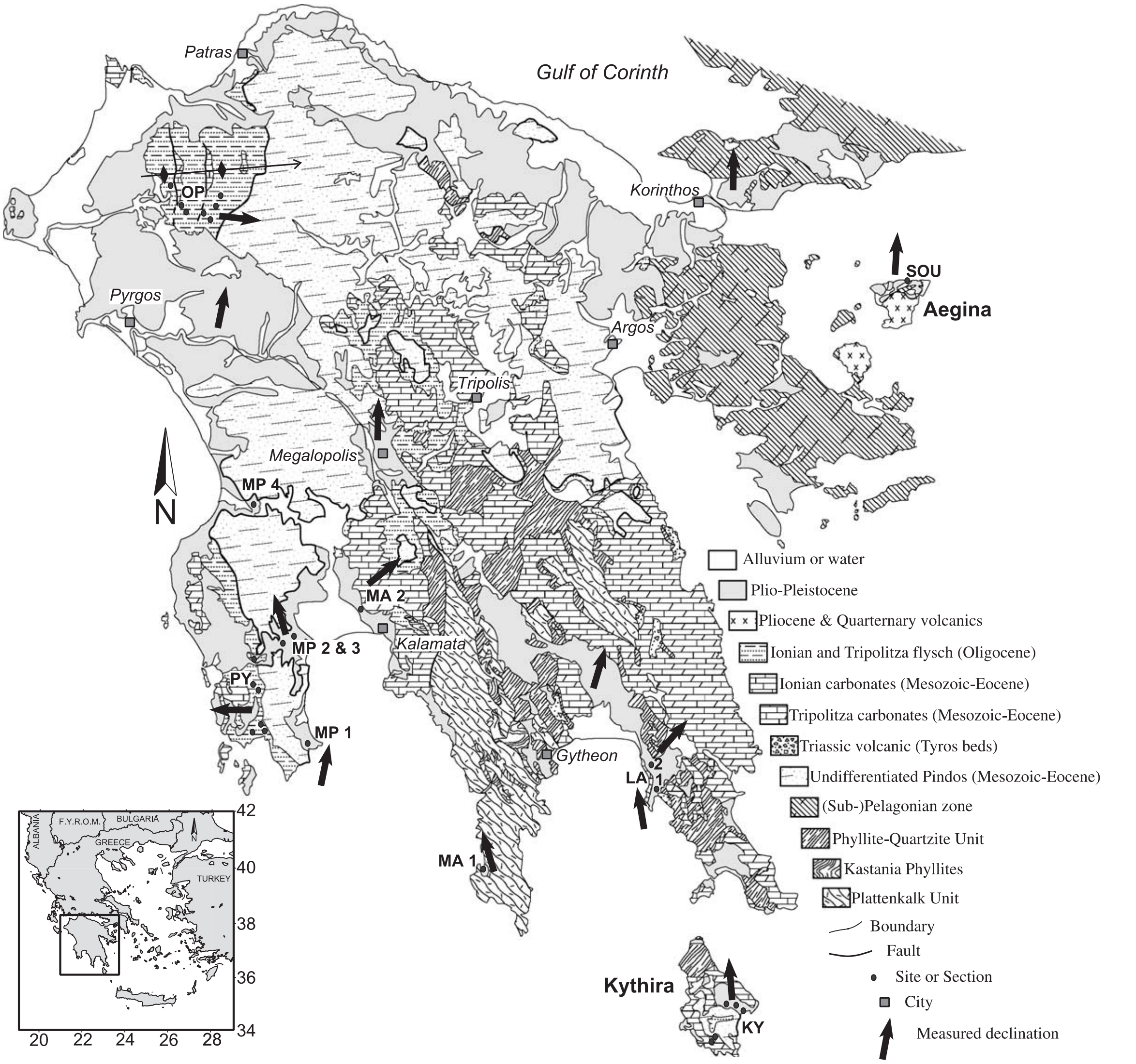

Fig. 4. Geologic map of southwestern Greece, modified after Bornovas and Rontogianni-Tsiabaou (1983) with sample locations and declination directions.

NE–SW striking right-lateral Thesprotiko shear zone was identified (Jordan et al., submitted for publication; Fig. 3), which is presently seismically inactive, but which once may have been connected to the Kefallonia Fault Zone.

The stratigraphy of the Ionian and Tripolitza Zones can generally be subdivided in a Mesozoic–Eocene series of limestones, overlain by a 1500- to 6000-m-thick deep-marine Oligocene clastic series of alternating clay and turbiditic sandstone layers (Ionian and Tripolitza flysch: e.g., Avramidis and Zelilidis, 2001; Avramidis et al., 2000, 2002; B.P. Co. Ltd., 1971; IGRS-IFP, 1966; Peeters et al., 1998; Wilpshaar, 1995). The age of the transition from carbonate to clastic sedimentation is estimated by Wilpshaar (1995) and Peeters et al. (1998) to be Earliest Oligocene (early Rupelian). The top of the carbonate sequence becomes more clay and silt rich and is generally followed by approximately five top 15 m of blue marl preceding the first turbiditic sandstones.

To assess the dimensions of the rotating domains, 12 localities, varying from 1 to 8 sites of 8 to 10 samples each (Fig. 3), were sampled in the basal 5 to 15 m of blue marls of the Ionian flysch.

To estimate the timing of the rotation of the various rotating domains, Neogene sediments were sampled. Lower Miocene clastic sediments were deposited in the Klematia–Paramythia Basin. These sediments are folded into the Botsara syncline (Avramidis et al., 2002; IGRS-IFP, 1966). Five sites and three long sections were sampled in the Lower Miocene of the Botsara-syncline [locality BO and sections Botsara West (BW)/Basin Plain (BP) and Botsara Top (BT) (all corresponding to section AA′ of Avramidis et al., 2000, 2002 and BE] and near Kryopigi (KP) and Kalamarina (KM; Fig. 3). In total, 13 outcrops of younger sediments were sampled: samples from the Middle Miocene were collected near Parga (PAP), from the Upper Miocene (Tortonian) on northwestern Corfu (CA) and the west coast of mainland Greece (PO and PA), and from the lower Pliocene of Corfu (CM, CAS, CL), Kefallonia (KS) and the west coast of mainland Greece (RZ; Fig. 3). Samples that were taken from the Corfu Coast section (CC) for magnetostratigraphy by Linssen (1991) were reevaluated for rotation analysis.

2.5. Peloponnesos, Kythira and Aegina (southwestern Greece)

A total of 259 cores was collected from 27 sites in southwestern Greece.

On the Peloponnesos, the nappe pile contains a tectonic window, which exposed the metamorphosed Phyllite–Quartzite and the Plattenkalk Units (Fig. 4). These units were exhumed in the Miocene (Bonneau, 1984; Jolivet et al., 1996; Theye and Seidel, 1991). Plio-Pleistocene extension formed a number of sedimentary basins (Benda et al., 1987; Frydas and Bellas, 1994; Hageman, 1977; Piper et al., 1976, 1982; Van Hinsbergen et al., submitted for publication(a); Van Vugt et al., 2001; Zelilidis and Doutsos, 1992; Zelilidis et al., 1988; Fig. 4).

In the northwest and southwest, two localities (OP and PY) were drilled in the lower Oligocene flysch for comparison with the Oligocene localities sampled in western Greece. Additionally, eight sites were sampled in the upper Plio-Pleistocene blue marls and silts of the south-Peloponnesos (MP, MA and LA-sites). On Aegina, paleomagnetic results were obtained from the Upper Miocene (Messinian) Souvala section, earlier sampled for magnetostratigraphy (Van Hinsbergen et al., 2004). On Kythira, five sites were drilled in the Upper Miocene (Tortonian) and Lower Pliocene marine sequences, in addition to the previously reported results of Duermeijer et al. (2000).

3. Paleomagnetic results

3.1. Characteristic Remanent Magnetisation (ChRM) directions

The paleomagnetic samples were taken with a water-cooled, generator-powered electric drill and oriented with a magnetic compass. The samples were either thermally demagnetised with small temperature increments of 20–80 °C up to a maximum temperature of 690 °C in a magnetically shielded, laboratory-built furnace, or progressively demagnetised in an alternating field (AF) with 5–50 mT increments up to 300 mT. The natural remanent magnetisation (NRM) of the specimens was measured on a 2G Enterprises horizontal DC SQUID cryogenic magnetometer.

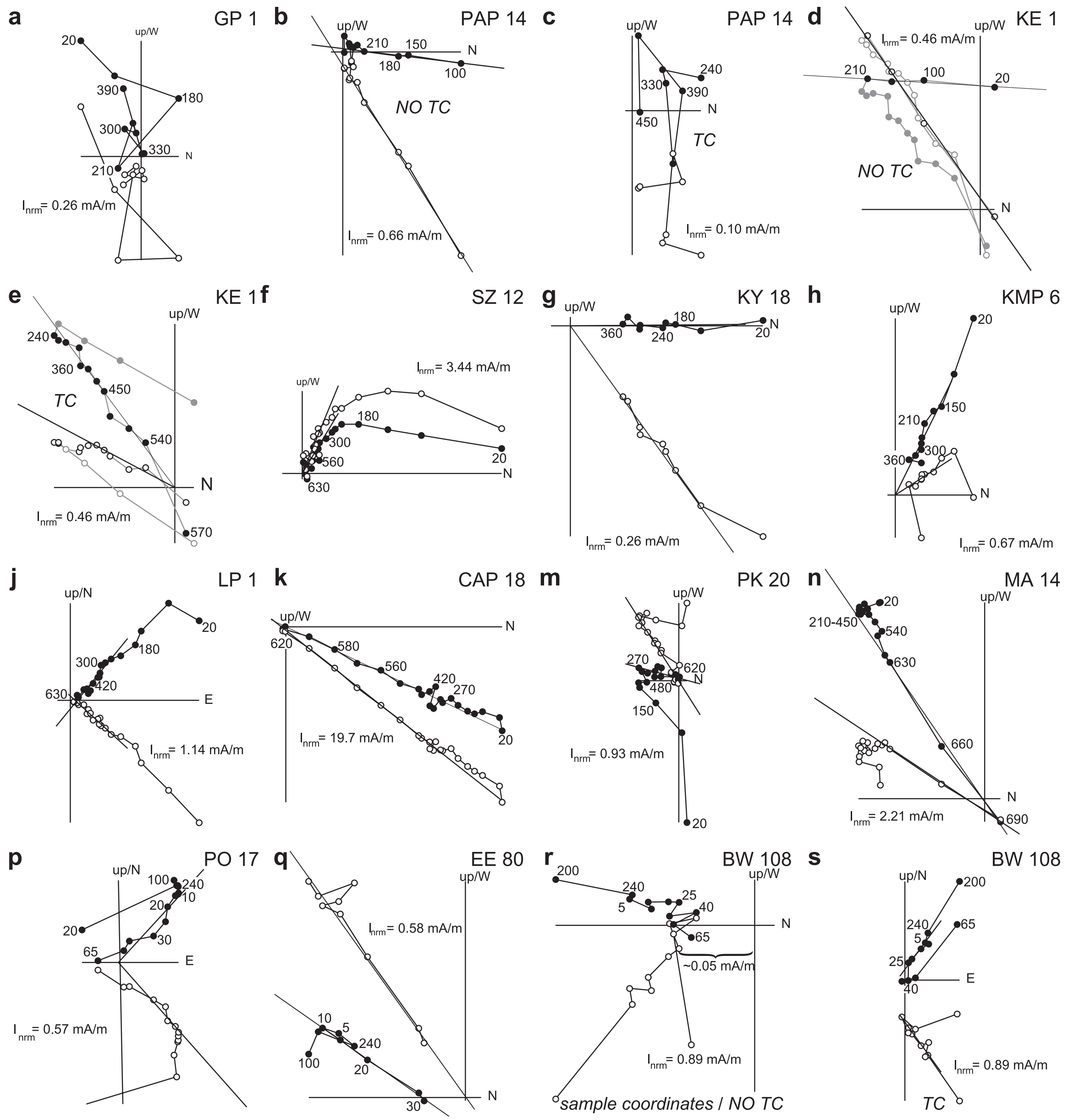

Fig. 5. Zijderveld diagrams (Zijderveld, 1967) of the analysed samples. (a) No sensible result from lower Oligocene clays; (b and c) strong present-day field overprint in middle Miocene marls; (d and e) present-day field overprint, leaving the ChRM after removal in lower Oligocene clays; (f) present-day field overprinting a reversed ChRM in lower Oligocene clays; (g) probably iron sulfide magnetisation showing normal polarity and no rotation in middle Pliocene marls; (h) magnetite magnetisation (see text) and reversed polarity and 110°cw rotation in lower Miocene clays; (j) magnetite/maghaemite magnetisation showing normal polarity and 45°cw rotation in lower Oligocene clays; (k) magnetite/maghaemite magnetisation showing normal polarity and 25°cw rotation in Tortonian clays; (m) magnetite/maghamite magnetisation showing reversed polarity and 50°cw rotation in lower Oligocene clays; (n) haematite magnetisation showing reversed polarity and 25° clockwise rotation in Pleistocene silts; (p) AF demagnetised Tortonian clays showing normal polarity and 50° clockwise rotation; (q) AF demagnetised upper Eocene/lower Oligocene clays showing reversed polarity and 30° clockwise rotation; (r and s) AF demagnetised lower Miocene clays showing the typical small-induced magnetisation (see text for further explanation).

Some low-intensity samples did not give a sensible result and were hence discarded (e.g., Fig. 5a). In most other cases, a normal polarity component is removed at temperatures between 100 and 210 °C (Fig. 5b–e), which is interpreted as a present-day field component. After removal of this component, in some cases, no sensible result is obtained (Fig. 5b and c). Alternatively, the original magnetisation may be (partly) overprinted (Fig. 5f) or one or more magnetic components are still present (Fig. 5d and e). In almost all specimens, a component with an unblocking temperature between

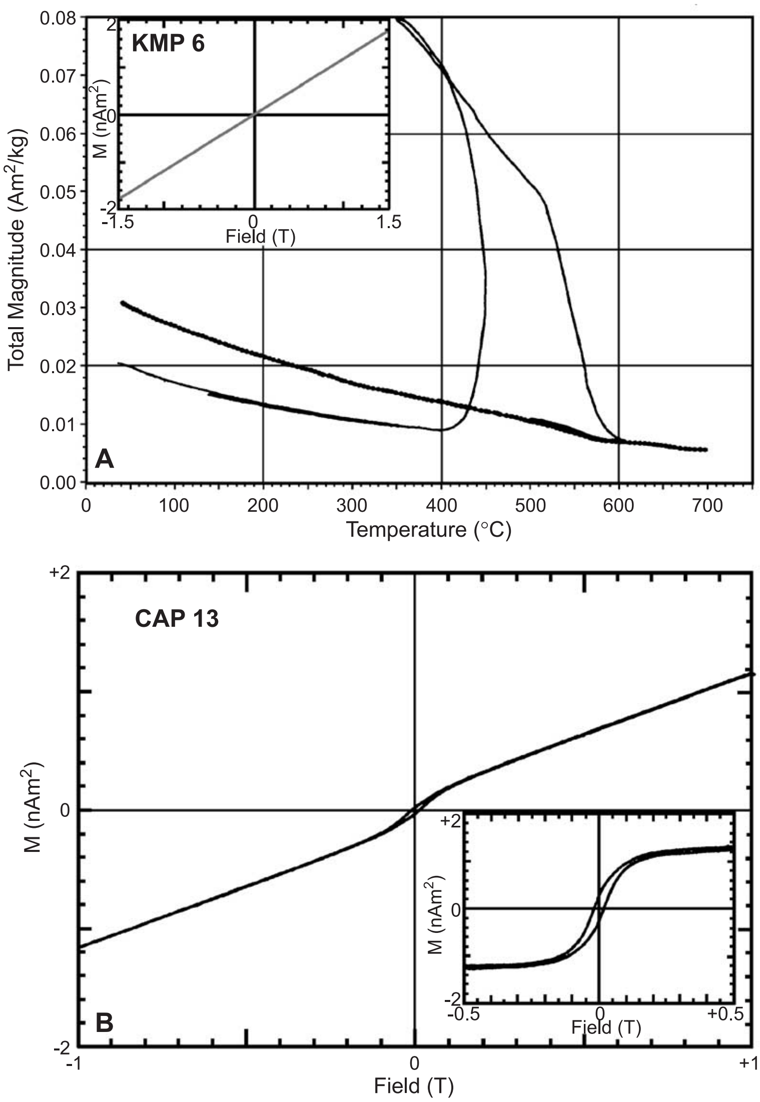

Fig. 6. Rock magnetic properties of samples can be divided in two major classes: (A) Thermomagnetic curves of marine marl samples show a predominantly paramagnetic component due to clay minerals, as suggested from the creation of a ferromagnetic phase above 400 °C. (B). Although still strongly influenced by paramagnetic behaviour, the majority of the samples show magnetite dominated hysteresis parameters, especially if corrected for the paramagnetic slope (inset). Typically, the coercive forces range 20–30 mT, further proving magnetite as the main carrier of the ChRM.

290 and 410 °C is present (Fig. 5g and h), suggesting iron sulphides as an important carrier of the magnetic signal. Thermomagnetic curves of marine marl samples show dominantly paramagnetic behaviour, likely because of the clay minerals, as can be seen from the typical paramagnetic decay until approximately 400 °C, as well as from the hysteresis loop (inset) in fields up to 1.5 T (Fig. 6A). Upon further heating, fine-grained magnetite is formed above 400 °C through oxidation of pyrite. The newly formed magnetite, evident from the maximum Curie temperature of approximately 580 °C, may cause spurious magnetisations during thermal demagnetisation (see Fig. 5h). Despite the dominantly paramagnetic behaviour, however, many samples—although of low remanent (ferromagnetic) intensity—give a reliable and consistent ChRM.

In addition, magnetite or maghaemite are present, indicated by unblocking temperatures of ~580 and ~625 °C, respectively (Fig. 5j, k and m) and the associated rock magnetic properties (Fig. 6B). In our samples, haematite—characterised by rapidly decreasing intensities between 630 and 670 °C—is only rarely the carrier of the magnetic signal (Fig. 5n).

Most of our samples with iron sulphides have low intensities, and thermal demagnetisation is not possible at temperatures exceeding 390–420 °C caused by breakdown of pyrite into magnetite (Fig. 6A); additional analysis was carried out on these samples using AF-demagnetisation. To remove the present-day field component, these samples were thermally demagnetised in three or four steps up to a temperature of 240 °C. Afterwards, increasing increments of 5–50 mT were applied until demagnetisation was completed (Fig. 5p and q).

Generally, the 240–390 °C, 570–625 °C and 5–300 mT components were considered to represent the Characteristic Remanent Magnetisation (ChRM). Occasionally, a small, induced magnetisation in the 2G Enterprises horizontal DC SQUID cryogenic magnetometer may result in a small deviation from the origin of the Zijderveld-diagrams, particularly in low-intensity samples. When results are plotted in sample coordinates, a typical deviation of approximately −0.05 mA/m is found (Fig. 5r and s). If the magnetic intensity of the sample is high, this deviation has no noticeable effect. If samples have low intensities and are susceptible to such induced magnetisation, the ChRM is determined excluding the origin (Fig. 5r and s).

After a ChRM direction was determined for all suitable cores of a site, a site mean was determined. First, the resulting ChRM directions were calculated without tectonic tilt correction (TC), to check if the measured direction corresponds to a present-day field direction. Additional criteria were based on a consistent decay of the NRM at temperatures exceeding 240 °C. Then, tectonic correction was carried out and the average site direction was calculated (Fig. 7a).

When a strong present-day field component was detected overlapping with the ChRM, we occasionally used great circles in addition to directly determined ChRM directions (McFadden and McElhinny, 1988; e.g., section Kedros–Sgourou on Kefallonia; Fig. 10).

The quality of the rotation estimated increases with increasing k-values and decreasing 95% confidence limits (Tables 1–3). We chose a minimum k-value of 20 and a minimum of four data points to consider an average as conclusive (type 1 measurement), since below these values, confidence limits are generally very high. The 95% confidence limits were further used to indicate the robustness of the type 1 measurements. If only one or two cores were suitable for interpretation, the site was considered inconclusive and not used (type 3 measurement). All other cases were used as a mere indication for the amount and sense of the rotation (type 2). After construction of the site averages, locality means were calculated using the same method. In the locality plots (Figs. 8–10) rotation with respect to the north pole is shown: from reversed sites, the antipodal normal direction was used.

Morris and Anderson (1996), following the suggestion of Kissel and Laj (1988), compared their data of Miocene granitoids of Naxos and Mykonos to the apparent polar wander path of Africa and applied a reference direction of D=005°, I=42° based on, e.g., Besse and Courtillot (1991). We did not apply such corrections for the following reasons. Kissel and Laj (1988) argued that throughout most of the Tertiary, the Aegean domain was attached to Africa and thus followed the polar wander path of Africa. At least since the latest

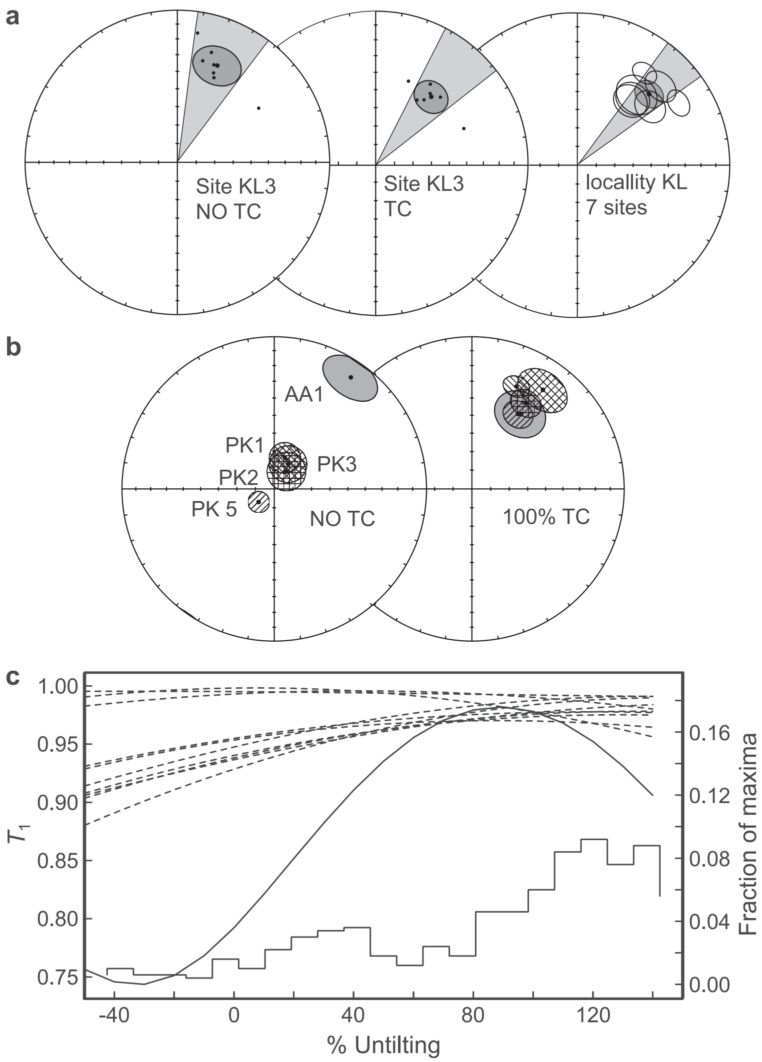

Fig. 7. (a) Site average after bedding tilt correction for individual sites and for the locality mean. (b) Positive fold test of localities AA and PK on the northeastern and southwestern limb, respectively, of a large syncline in northern Epirus (see Fig. 3 for locations). (c) Diagram after Tauxe and Watson (1994), showing that at 89% unfolding the best match is obtained between the sites of localities AA and PK.

Oligocene, when the Tripolitza and Ionian zones in the external Hellenides started to be severely deformed, these zones are incorporated in the accetionary wedge, i.e., Europe. The Mesohellenic trench developed as a foreland basin of the Pindos fold and thrust belt (e.g., Doutsos et al., 1994) and was thus never part of Africa. In an accretionary wedge, the 'affinity' of the various units with the underriding and overriding plate varies rapidly through time and space. Moreover, the age calibration of the sediments, especially for the younger Neogene, is much more accurate than for the polar wander paths and it is therefore difficult to assess which sites should or should not be corrected.

Some data sets that have been published are corrected, some are not and not all sets were corrected by the same values. As a result, the published rotation values may vary by approximately 5°.

In some cases, a reversal test could be carried out. Although the inclination in the Mesohellenic Basin in

Table 1
Results of NRM analyses from the sites and sections of northern Greece, corrected for bedding tilt

Locality	Samples	Na	Nc	q	Decl	Incl	*k*	α95	Pol	Rot		Age (reference)
Mesohellenic Basin, RT: class C, y=14.9>yc=15.9												
Klimataki	KH 1–10	10	4	3	355.8	53.7	11.5	28.3	N	4	ccw	E. Pliocene (Fountoulis et al., 2001)
EE	mean		6		51.7	28.2	19.5	15.5	N/R	52	cw	Oligocene–M. Miocene (Fountoulis et al., 2001)
Eptachorio	mean		4	2	65.4	39.1	15.3	24.3	N/R	65	cw	L. Eocene–Oligocene (Avramidis et al., 2002; Bornovas and Rontogianni-Tsiabaou, 1983)
EE 1	EE 1–10	10		3	–	–	–	–	–	–	–	L. Eocene–Oligocene (Avramidis et al., 2002; Bornovas and Rontogianni-Tsiabaou, 1983)
EE 2	EE 11–20	10	10	1	75.1	37.6	27.8	9.3	N	75	cw	L. Eocene–Oligocene (Avramidis et al., 2002; Bornovas and Rontogianni-Tsiabaou, 1983)
EE 3	EE 21–30	10		3	–	–	–	–	–	–	–	L. Eocene–Oligocene (Avramidis et al., 2002; Bornovas and Rontogianni-Tsiabaou, 1983)
EE 4	EE 31–40	10	–	3	–	–	–	–	–	–	–	L. Eocene–Oligocene (Avramidis et al., 2002; Bornovas and Rontogianni-Tsiabaou, 1983)
EE 5	EE 41–50	10	6	1	215.5	−22.5	20.5	15.2	R	36	cw	L. Eocene–Oligocene (Avramidis et al., 2002; Bornovas and Rontogianni-Tsiabaou, 1983)
EE 6	EE 51–60	10	8	1	42.0	31.5		11.3	N	42	cw	L. Eocene–Oligocene (Avramidis et al., 2002; Bornovas and Rontogianni-Tsiabaou, 1983)
EE 7	EE 61–70	10	10	1	47.9	47.7		14.6	N	48	cw	L. Eocene–Oligocene (Avramidis et al., 2002; Bornovas and Rontogianni-Tsiabaou, 1983)
Sites along section EE												
EE 8	EE 71–80	8	1	3	220.0	−49.0			R	40	cw	Oligocene–M. Miocene (Avramidis et al., 2002)
EE 12	EE 111–120	10	7	1	234.3	−9.1	14.2	18.4	R	54	cw	Oligocene–M. Miocene (Avramidis et al., 2002)
EE 13	EE 121–128	8	8	1	237.1	−17.7	261.9	4.1	R	57	cw	Oligocene–M. Miocene (Avramidis et al., 2002)
EE 11	EE 101–110	10		3	–	–	–	–	–	–	–	Oligocene–M. Miocene (Avramidis et al., 2002)
EE 10	EE 91–100	10		3	–	–	–	–	–	–	–	Oligocene–M. Miocene (Avramidis et al., 2002)
EE 9	EE 81–90	10		3	–	–	–	–	–	–	–	Oligocene–M. Miocene (Avramidis et al., 2002)
DD	mean		8	1	51.0	20.3	25.8	11.1	N/R	51	cw	Oligocene–M. Miocene (Avramidis et al., 2002)
Krania	mean		6	1	46.4	19.5	27.2	13.1	N/R	46	cw	L. Eocene (Avramidis et al., 2002; Bornovas and Rontogianni-Tsiabaou, 1983)
DD 1	DD 1–10	10	8	1	45.9	24.8		14.5	N	46	cw	L. Eocene (Avramidis et al., 2002; Bornovas and Rontogianni-Tsiabaou, 1983)
DD 2	DD 11–20	10	6	1	59.7	18.4		7.9	N	60	cw	L. Eocene (Avramidis et al., 2002; Bornovas and Rontogianni-Tsiabaou, 1983)

Table 1 (*continued*)

Locality	Samples	Na	Nc	q	Decl	Incl	*k*	α95	Pol	Rot		Age (reference)
DD 3	DD 21–30	10	4	2	245.8	−22.8		21.2	R	66	cw	L. Eocene (Avramidis et al., 2002; Bornovas and Rontogianni-Tsiabaou, 1983)
DD 4	DD 31–40	10	6	1	218.9	−8.6	12.3	19.9	R	39	cw	L. Eocene (Avramidis et al., 2002; Bornovas and Rontogianni-Tsiabaou, 1983)
DD 5	DD 41–50	10	7	1	208.7	−30.2		15.8	R	29	cw	L. Eocene (Avramidis et al., 2002; Bornovas and Rontogianni-Tsiabaou, 1983)
DD 6	DD 51–60	10	9	1	279.2	−23.1		13.7	R	109*	cw	L. Eocene (Avramidis et al., 2002; Bornovas and Rontogianni-Tsiabaou, 1983)
DD 7	DD 61–70	10	10	1	218.9	−9.7	32.5	8.6	R	39	cw	L. Eocene (Avramidis et al., 2002; Bornovas and Rontogianni-Tsiabaou, 1983)
Sites along section DD												
DD 8	DD 71–80	10	9	1	251.2	−16.8	36.6	8.6	R	71	cw	Oligocene–M. Miocene (Avramidis et al., 2002; Bornovas and Rontogianni-Tsiabaou, 1983)
DD 9	DD 81–87	7	7	1	58.3	26.8	13.8	16.8	N	58	cw	Oligocene–M. Miocene (Avramidis et al., 2002; Bornovas and Rontogianni-Tsiabaou, 1983)
Florina–Ptolemais–Servia Basin			7		9.8	50.2	238.3	3.9		10	cw	4.0 Ma
Vegora	section mean				10.2	46.0				10	cw	6.0 Ma (Steenbrink, 2001)
RT: class B, y=4.3>yc=8.0	normal		7	1	11.8	51.3	27.5	11.7	N	12	cw	
	reversed		36	2	188.5	−40.6	18.5	5.7	R	9	cw	
Anagyri	section mean				190.1	−45.9	20.4	11.7		10	cw	Lower Pliocene (Bornovas and Rontogianni-Tsiabaou, 1983; Van Vugt et al., 1998)
	normal		2	2	2.6	60.8	–	–	N	3	cw	
	reversed		9	1	190.1	−45.9	20.4	11.7	R	10	cw	
Vorio	section mean				8.6	51.1				9	cw	4.0 Ma (Van Vugt et al., 1998)
RT: class B, y=4.3>yc=8.0	normal		18	1	11.3	49.9	20.1	7.9	N	11	cw	
	reversed		76	1	185.7	−52.3	23.1	3.5	R	6	cw	
Komanos	section mean				2.3	56.4				2	cw	5.0 Ma (Steenbrink, 2001; Van Vugt et al., 1998)
RT: class A, y=1.9>yc=3.9	normal		85	1	2.1	57.3	39.6	2.5	N	2	cw	
	reversed		71	1	182.4	−55.4	31.8	3.0	R	2	cw	
Tomea Eksi	section mean				9.1	54.9				9	cw	5.0 Ma (Steenbrink, 2001; Van Vugt et al., 1998)
RT: class A, y=1.6>yc=3.8	normal		57	1	8.1	55.4	38.6	3.1	N	8	cw	
	reversed		130	1	190.1	−54.3	29.3	2.3	R	10	cw	
Lava	section mean				17.1	51.6				17	cw	6.2 Ma (Steenbrink et al., 2000)
RT: class A, y=1.1>yc=4.3	normal		81	1	17.5	52.1	44.1	2.4	N	18	cw	
	reversed		66	1	196.6	−51.2	27.6	3.4	R	17	cw	
Prosilio	section mean				9.9	45.3				10	cw	5.2 Ma (Van Vugt et al., 1998)

(continued on next page)

Table 1 (*continued*)

Locality	Samples	Na	Nc	q	Decl	Incl	*k*	α95	Pol	Rot		Age (reference)
RT: Indet. y=19.5>yc=8.3	normal		34	1	11.8	55.0	41.7	3.9	N	12	cw	
	reversed		25	2	188.0	−35.7	15.9	7.5	R	8	cw	
Strimon Basin	mean		1		1.1	43.2			N/R	1	cw	L. Miocene (Snel et al., in press)
Kavala Road section	KR		9	2	58.4	40.7	7.6	20.0	N	58	cw	Early Pliocene (Snel et al., in press)
Labyrinthos section	LA		14	1	359.1	40.6	39.1	6.4	N	1	ccw	L. Miocene (Messinian) (Snel et al., in press)
			8	1	183.1	−45.8	40.9	8.8	R	3	cw	L. Miocene (Messinian) (Snel et al., in press)
Lefkon section	LF		3	2	190.2	−39.1	14.2	34.0	R	10	cw	L. Miocene (L. Valesian) (Armour-Brown et al., 1979)
Myrini section	MY		8	2	166.5	−48.3	7.4	21.7	R	13	ccw	E. Miocene (Snel et al., in press; Armour-Brown et al., 1979)
Rema Marmara section	RM		0	3	–	–	–	–	–	–	–	E. Pliocene (Snel et al., in press)

Na=number of analysed samples, Nc=number of conclusive samples, q=quality (1=conclusive, 2=indicative, 3=inconclusive), Decl=declination, Incl=inclination, *k*=Fisher's precision parameter (Fisher, 1953), α95=95% cone of confidence, pol=polarity, rot=amount of rotation, sense=sense of rotation (cw=clockwise, ccw=counterclockwise).

Table 2
Results of NRM analyses from the sites and sections of (north)western Greece, corrected for bedding tilt

Locality	Samples	Na	Nc	q	Decl	Incl	*k*	α95	Pol	Rot		Age (reference)
EPIRUS												
Konitsa–Exochi			1		232.9	−26.0	39.6	12.3	R	53	cw	Oligocene (IGRS-IFP, 1966)
KE 1	KE 1–5	5	5	2	232.9	−26.0	39.6	12.3	R	53	cw	Oligocene (IGRS-IFP, 1966)
KE 2	KE 11–13	3	0	3	–	–	–	–	–	–		Oligocene (IGRS-IFP, 1966)
Paleopyrgos												
PP 1	PP 1–2	2	0	3	–	–	–	–	–	–		Oligocene (IGRS-IFP, 1966)
Palamba–Kerasochori			4		30.9	31.1	68.9	11.1	N/R	31	cw	Oligocene (IGRS-IFP, 1966)
PK 1	PK 1–10	10	8	1	24.1	27.9	79.5	6.3	N	24	cw	Oligocene (IGRS-IFP, 1966)
PK 2	PK 11–20	10	8	1	212.2	−33.7	53.8	7.7	R	32	cw	Oligocene (IGRS-IFP, 1966)
PK 3	PK 21–30	10	7	1	35.7	21.0	26.5	12.0	N	36	cw	Oligocene (IGRS-IFP, 1966)
PK 4	PK 31–40	10	10	1	43.6	−32.2	20.1	11.0	R	224	cw	Oligocene (IGRS-IFP, 1966)
PK 5	PK 41–49	9	9	1	211.7	−41.7	48.0	7.5	R	32	cw	Oligocene (IGRS-IFP, 1966)
Ag. Nikolaos–Ag. Pandes			1		32.8	40.9			N	33	cw	Oligocene (IGRS-IFP, 1966)
AA 1	AA 1–10	10	4	1	32.8	40.9	50.9	13.0	N	33	cw	Oligocene (IGRS-IFP, 1966)
AA 2	AA 11–20	10	7	2	154.7	−32.0	16.7	15.2	R	25*	ccw	Oligocene (IGRS-IFP, 1966)
Saloniki–Zalongo	mean		1		58.4	41.3			N	58	cw	E. Oligoc. (Rupelien) (Peeters et al., 1998)
SZ 1	SZ 1–10	7	5	1	58.4	41.3	33.9	13.3	N	58	cw	E. Oligocene (Rupelien) (Peeters et al., 1998)

Table 2 (*continued*)

Locality	Samples	Na	Nc	q	Decl	Incl	*k*	α95	Pol	Rot		Age (reference)
SZ 2	SZ 11–20	10	8	1	305.1	−41.7	45.1	8.3	R	135*	cw	E. Oligocene (Rupelien) (Peeters et al., 1998)
SZ 3	SZ 21–30	10	5	2	33.7	36.2	48.4	11.1	N	34*	cw	E. Oligocene (Rupelien) (Peeters et al., 1998)
			5	2	292.2	−44.1	6.1	33.6	R	112*	cw	E. Oligocene (Rupelien) (Peeters et al., 1998)
SZ 4	SZ 31–40	10	0	3	–	–	–	–	R	–		E. Oligocene (Rupelien) (Peeters et al., 1998)
SZ 5	SZ 41–49	9	0	3	–	–	–	–	R	–		E. Oligocene (Rupelien) (Peeters et al., 1998)
SZ 6	SZ 51–60	10	10	1	282.4	−24.6	79.7	5.4	R	102*	cw	E. Oligocene (Rupelien) (Peeters et al., 1998)
SZ 7	SZ 61–70	10	0	3	–	–	–	–	R	–		E. Oligocene (Rupelien) (Peeters et al., 1998)
Gourpanitsa–Polygiros												
GP 1	GP 1–10	10	5	2	221.0	−40.9	12.8	26.7	R	41	cw	Oligocene (IGRS-IFP, 1966)
Botsara Syncline	mean		7		61.3	42.6	35.7	10.2	N/R	61	cw	E. Miocene (IGRS-IFP, 1966)
Sites	mean		4		71.2	44.0	57.3	12.2	N/R	71	cw	E. Miocene (IGRS-IFP, 1966)
BO 1	BOP 1–10	10	7	2	239.1	−35.4	14.3	16.5	N/R	59	cw	E. Miocene (IGRS-IFP, 1966)
BO 2	BOP 11–20	10	6	1	101.8	52.8	21.2	14.9	N	102*	cw	E. Miocene (IGRS-IFP, 1966)
BO 3	BOP 21–30	10	10	1	82.9	38.9	35.0	8.3	N	83	cw	E. Miocene (IGRS-IFP, 1966)
BO 4	BOP 31–39	9	9	1	74.2	49.2	47.9	7.5	N	74	cw	E. Miocene (IGRS-IFP, 1966)
BO 5	BOP 41–49	9	7	1	69.1	51.0	33.7	10.5	N	69	cw	E. Miocene (IGRS-IFP, 1966)
Sections	mean		3	1	48.9	39.5	49.9	17.6	N/R	49	cw	E. Mioc. (Burdigalian) (Van Hinsbergen et al., submitted for publication(b))
Botsara East	BE 1–47	47	2	1	220.7	−27.2			R	41	cw	E. Mioc. (Burdigalian) (Van Hinsbergen et al., submitted for publication(b))
Botsara West	BW 1–138	114	41	2	41.3	44.0	11.0	7.0	N	41	cw	E. Mioc. (Burdigalian) (Van Hinsbergen et al., submitted for publication(b))
Basin Plain	BP 1–25	15	10	1	227.9	−28.2	31.9	8.7	R	48	cw	E. Mioc. (Burdigalian) (Van Hinsbergen et al., submitted for publication(b))
			2	2	25.0	31.6			N	25	cw	E. Mioc. (Burdigalian) (Van Hinsbergen et al., submitted for publication(b))
Botsara Top	BT 1–62	60	36	2	61.4	48.8	16.7	6.0	N	61	cw	E. Mioc. (Burdigalian) (Van Hinsbergen et al., submitted for publication(b))
Parga												
PA 1	PA 1–18	16	7	1	30.4	28.1	46.6	8.9	N/R	30	cw	Middle Miocene (Bizon et al., 1983)
Nicolitsi II, IV, V			3		85.4	34.7	25.0	5.9		85	cw	Oligocene (IGRS-IFP, 1966)
NI 1	NI 1–10	10	10	1	48.8	36.0	151.1	3.9	N	49	cw	Oligocene (IGRS-IFP, 1966)
NI 2	NI 11–20	10	8	1	80.2	20.9	1071.9	1.7	N	80	cw	Oligocene (IGRS-IFP, 1966)
NI 3	NI 21–30	10	9	1	344.8	42.6	22.3	11.1	N	14*	cw	Oligocene (IGRS-IFP, 1966)
NI 4	NI 31–40	10	8	1	273.1	−35.5	27.7	10.7	R	93	cw	Oligocene (IGRS-IFP, 1966)
NI 5	NI 41–49	9	9	1	264.0	−46.2	36.1	8.7	R	84	cw	Oligocene (IGRS-IFP, 1966)
Seriziana–Alepochori												
SA 1	SAP 1–6	6	0	3	–	–	–	–	–	–	–	Oligocene (IGRS-IFP, 1966)

(*continued on next page*)

Table 2 (*continued*)

Locality	Samples	Na	Nc	q	Decl	Incl	*k*	α95	Pol	Rot		Age (reference)
Kryopigi	mean		3		39.3	50.0	40.3	19.7	N	39	cw	E. Miocene (IGRS-IFP, 1966)
KP 1	KPP 1–10	10	8	2	219.3	16.1	8.4	20.3	R	39	cw	E. Miocene (IGRS-IFP, 1966)
KP 2	KPP 11–20	10	8	2	32.1	50.3	13.8	15.5	N	32	cw	E. Miocene (IGRS-IFP, 1966)
KP 3	KPP 21–30	10	7	2	25.5	47.1	13.9	16.8	N	26	cw	E. Miocene (IGRS-IFP, 1966)
KP 4	KPP 31–39	8	7	2	62.0	49.4	19.7	14.0	N	62	cw	E. Miocene (IGRS-IFP, 1966)
KP 5	KPP 41–50	10	0	3	–	–	–	–	R	–	–	E. Miocene (IGRS-IFP, 1966)
Ekklissia [4]	EKL	3	3	2	283.5	−36.7	9.8	41.6	R	104*	cw	Oligocene (Wilpshaar, 1995)
Kalamarina												
KM 1	KMP 1–10	10	8	1	287.7	−30.5	51.8	7.8	R	118	cw	E. Miocene (IGRS-IFP, 1966)
Riza	RZ 1–40	40	3	2	24.2	42.3	11.5	38.1	N	24	cw	Early Pliocene (Van Hinsbergen et al., submitted for publication(a))
			18	2	233.9	−37.9	11.9	12.0	R	54	cw	Early Pliocene (Van Hinsbergen et al., submitted for publication(a))
Kalentzi–Lazena	mean		8		45.4	34.0	58.7	7.3	N	45	cw	Oligocene (IGRS-IFP, 1966)
KL 1	KL 1–10	10	9	1	51.2	38.8	39.2	8.3	N	51	cw	Oligocene (IGRS-IFP, 1966)
KL 2	KL 11–20	10	10	1	39.4	44.1	31.2	8.8	N	39	cw	Oligocene (IGRS-IFP, 1966)
KL 3	KL 21–29	9	7	1	39.9	42.5	47.7	8.8	N	40	cw	Oligocene (IGRS-IFP, 1966)
KL 4	KL 31–39	9	9	1	46.6	25.6	41.7	8.1	N	47	cw	Oligocene (IGRS-IFP, 1966)
KL 5	KL 41–50	10	10	1	40.3	39.3	21.7	10.6	N	40	cw	Oligocene (IGRS-IFP, 1966)
KL 6	KL 51–60	10	9	1	58.3	22.6	67.8	6.3	N	58	cw	Oligocene (IGRS-IFP, 1966)
KL 7	KL 61–70	10	8	1	35.8	25.9	87.2	6.0	N	36	cw	Oligocene (IGRS-IFP, 1966)
Arakhtos (AR) [2]	PAR		7	1	229.3	−31.1	37.4	10.0	R	49	cw	E. Oligocene (Rupelien) (Peeters et al., 1998)
Limni Pournarion	mean		7	1	53.3	35.7	84.2	6.6	N/R	53	cw	Oligocene (IGRS-IFP, 1966)
LP 1	LP 1–8	8	8	2	60.0	41.6	16.8	13.9	N	60	cw	Oligocene (IGRS-IFP, 1966)
LP 2	LP 11–20	10	8	1	37.5	29.8	33.8	9.7	N	38	cw	Oligocene (IGRS-IFP, 1966)
LP 3	LP 21–29	9	8	1	236.7	−35.6	37.7	9.1	R	57	cw	Oligocene (IGRS-IFP, 1966)
LP 4	LP 31–40	10	10	1	246.0	−31.0	34.2	8.4	R	66	cw	Oligocene (IGRS-IFP, 1966)
LP 5	LP 41–49	9	9	1	50.6	34.7	34.9	8.8	N	51	cw	Oligocene (IGRS-IFP, 1966)
LP 6	LP 51–60	10	10	1	51.9	33.1	151.3	3.9	N	52	cw	Oligocene (IGRS-IFP, 1966)
LP 7	LP 61–70	10	8	1	51.3	41.9	100.4	5.6	N	51	cw	Oligocene (IGRS-IFP, 1966)
Northern Tripolitza			2		57.4	35.2			N/R	57	cw	Oligocene (IGRS-IFP, 1966)
NT 1	NT 1–10	10	9	1	39.8	32.0	28.2	9.9	N	40	cw	Oligocene (IGRS-IFP, 1966)
NT 2	NT 11–20	10	7	2	254.9	−35.7	11.2	18.8	R	75	cw	Oligocene (IGRS-IFP, 1966)
NT 3	NT 21–22	2	1	3	243.2	−44.4	–	–	R	63	cw	Oligocene (Fountoulis et al., 2001)
Paleros	PA 1–35	35	31	1	35.5	41.1	48.9	3.7	N	36	cw	L. Miocene (Tortonian) (Van Hinsbergen et al., submitted for publication(a))
Pogonia	PO 1–70	70	27	1	50.3	47.9	17.0	7.0	N	50	cw	L. Miocene (Tortonian) (Van Hinsbergen et al., submitted for publication(a))
			4	2	214.5	−27.6	36.5	15.4	R	35	cw	L. Miocene (Tortonian) (Van Hinsbergen et al., submitted for publication(a))
Southern Akarnania												
Mount Thiamo 1	MTC 1–10	10	1	3	309.6	36.3	–	–	N	50	cw	Oligocene (IGRS-IFP, 1966)
Mount Thiamo 2	MTC 11–18	8	–	3	–	–	–	–	R	–	–	Oligocene (IGRS-IFP, 1966)
Karavouna	KVC 1–7	7	2	3	–	–	–	–	N/R	–	–	Oligocene (IGRS-IFP, 1966)
Dimos Mesolongi	DMC 1–8	8	6	2	46.9	41.1	8.8	23.9	N	47	cw	Oligocene (IGRS-IFP, 1966)

Table 2 (*continued*)

Locality	Samples	Na	Nc	q	Decl	Incl	*k*	α95	Pol	Rot		Age (reference)
Corfu	mean		4		359.4	42.6	198.7	6.5	N/R	1	ccw	Early Pliocene (Van Hinsbergen et al., submitted for publication(a))
Monastery section	CMP 1–39	39	12	2	355.9	52.8	16.7	11.5	N	4	ccw	Early Pliocene (Van Hinsbergen et al., submitted for publication(a))
			11	2	179.8	−41.7	12.1	13.0	R	0		Early Pliocene (Van Hinsbergen et al., submitted for publication(a))
Lefkimmi 1	CLP 1–14	14	8	1	171.6	−43.7	23.9	11.6	R	8	ccw	Early Pliocene (Van Hinsbergen et al., submitted for publication(a))
Lefkimmi 2	CLP 15–28	14	0	3	–	–	–	–	R	–	–	Early Pliocene (Van Hinsbergen et al., submitted for publication(a))
Lefkimmi 3	CLP 29–35	7	0	3	–	–	–	–	R	–	–	Early Pliocene (Van Hinsbergen et al., submitted for publication(a))
Arillas Beach section	CAP 1–35	35	10	1	357.7	46.7	17.0	12.1	N	2	ccw	L. Miocene (Tortonian) (Van Hinsbergen et al., submitted for publication(a))
			3	2	163.9	−32.0	49.3	17.7	R	16	ccw	L. Miocene (Tortonian) (Van Hinsbergen et al., submitted for publication(a))
Aghios Stefanos	CASP 1–7	6		3	–	–	–	–	N	–	–	Early Pliocene (Van Hinsbergen et al., submitted for publication(a))
Corfu Coast section	mean		127	1	8.9	45.7	24.6	2.6	N/R	9	cw	Early Pliocene (Linssen, 1991)
RT: class A, y=3.2>yc=5.6	CA 1–100		55	1	8.3	46.0	27.6	3.2	N	8	cw	Early Pliocene (Linssen, 1991)
			75	2	192.8	−46.7	15.2	5.1	R	13	cw	Early Pliocene (Linssen, 1991)
Kefallonia												
Kedros–Sgourou	KS	13	10	2	89.5	28.3		10.2	N	90	cw	Early Pliocene (Van Hinsbergen et al., submitted for publication(a))

Na=number of analysed samples, Nc=number of conclusive samples, q=quality (1=conclusive, 2=indicative, 3=inconclusive), decl=declination, incl=inclination, *k*=Fisher's precision parameter (Fisher, 1953), α95=95% cone of confidence, pol=polarity, rot=amount of rotation, sense=sense of rotation (cw=clockwise, ccw=counterclockwise).

all sites is much lower than would be expected for the present latitude of Greece, the reversal test (McFadden and McElhinny, 1990) turned out positive (Fig. 8, Table 1). The reversal tests for most of the sections in the Florina–Ptolemais–Servia Basin were positive (Fig. 8, Table 1). Additionally, a positive result was obtained from a reversal test, carried out on the Corfu Coast section directions.

The localities Palamba–Kerasochori (PK) and Aghios Nikolaos–Aghios Pandes (AA) were sampled on the opposite limbs of a syncline and both the fold test of McFadden (1990) and Tauxe and Watson (1994) were successful (Fig. 7b and c). The resulting plots and values are listed in Figs. 8–10 and Tables 1–3.

4. Regional versus local rotations and their timing

To translate the rotations obtained for each section and site into locality-wide rotations, the following steps were taken. Anomalous declinations with respect to other sites within the same locality are

Table 3
Results of NRM analyses from the sites and sections of southwestern Greece, corrected for bedding tilt

Locallity	Samples	Na	Nc	q	Decl	Incl	*k*	α95	Pol	Rot	Sense	Age (reference)
Aegina												
Souvala section	SOU		11	1	182.8	−51.8	35.7	7.7	R	3	cw	5.5 Ma (Van Hinsbergen et al., 2004; Rögl et al., 1991)
Kythira	mean		6		355.2	47.4	35.8	11.3	N	5	ccw	Middle Pliocene (Steenbrink, 2001)
KY 1	KY 1–10	10		3	–	–	–	–	–	–	–	Tortonian (Meulenkamp et al., 1977)
KY 2	KY 11–20	10	9	1	5.4	58.0	97.1	4.9	N	5	cw	L. Pliocene (Van Hinsbergen et al., submitted for publication(a))
KY 3	KY 21–30	10	10	1	350.9	34.0	40.1	8.2	N	9	ccw	L. Pliocene (Van Hinsbergen et al., submitted for publication(a))
KY 4	KY 31–40	10	10	1	356.7	36.1	67.1	5.9	N	3	ccw	Tortonian (Meulenkamp et al., 1977)
KY 5	KY 41–50	10	7	1	4.7	51.8	90.7	5.8	N	5	cw	Tortonian (Meulenkamp et al., 1977)
Avlemonas [20]	AV		8	1	341.1	63.7	45.5	8.5	N	19	ccw	L. Pliocene (Meulenkamp et al., 1977; Duermeijer et al., 2000)
Kapsali [20]	KAP		12	1	351.9	39.4	29.7	8.1	N	8	ccw	L. Pliocene (Meulenkamp et al., 1977; Duermeijer et al., 2000)
Peloponnesos												
Olymbia–Patras	mean		3		96.3	32.6	25.3	25.0	N/R	96	cw	Oligocene (Bornovas and Rontogianni-Tsiabaou, 1983)
OP 1	OP 1–10	10	–	3	–	–	–	–				Oligocene (Bornovas and Rontogianni-Tsiabaou, 1983)
OP 2	OP 11–20	10	–	3	–	–	–	–				Oligocene (Bornovas and Rontogianni-Tsiabaou, 1983)
OP 3	OP 21–29	9	–	3	–	–	–	–				Oligocene (Bornovas and Rontogianni-Tsiabaou, 1983)
OP 4	OP 31–40	10	8	1	271.7	−31.3	54.2	6.6	R	92	cw	Oligocene (Bornovas and Rontogianni-Tsiabaou, 1983)
OP 5	OP 41–50	10	5	1	274.4	−18.0	15.5	20.1	R	94	cw	Oligocene (Bornovas and Rontogianni-Tsiabaou, 1983)
OP 6	OP 51–60	10	4	1	104.9	48.3	25.9	18.4	N	105	cw	Oligocene (Bornovas and Rontogianni-Tsiabaou, 1983)
OP 7	OP 61–70	10	–	3	–	–	–	–	R			Oligocene (Bornovas and Rontogianni-Tsiabaou, 1983)
Pylos	mean		–		–	–			–	–	–	Oligocene (Bornovas and Rontogianni-Tsiabaou, 1983)
PY 2	PY 11–17	7	0	3	273.9	10.0	88.5	7.2	N	94	ccw	Oligocene (Bornovas and Rontogianni-Tsiabaou, 1983)
PY 3	PY 21–25	5	0	3	–	–	–	–	–	–	–	Oligocene (Bornovas and Rontogianni-Tsiabaou, 1983)
PY 4	PY 31–40	10	0	3	–	–	–	–	–	–	–	Oligocene (Bornovas and Rontogianni-Tsiabaou, 1983)
PY 5	PY 41–50	10	0	2	–	–	–	–	–	–	–	Oligocene (Bornovas and Rontogianni-Tsiabaou, 1983)
PY 6	PY 51–57	7	0	3	89.8	−23.8	38.9	20.0	R	90	ccw	Oligocene (Bornovas and Rontogianni-Tsiabaou, 1983)
PY 7	PY 61–70	10	0	2	–	–	–	–	–	–	–	Oligocene (Bornovas and Rontogianni-Tsiabaou, 1983)
Laconia Peninsula												
LA 1	LA 1–10	10	4	2	170.4	−38.3	59.3	12.0	N	10	ccw	Plio/Pleistocene (Frydas, 1993)

Table 3 (*continued*)

Locallity	Samples	Na	Nc	q	Decl	Incl	*k*	α95	Pol	Rot	Sense	Age (reference)
LA 2	LA 11–20	10	10	2	221.0	−34.1	11.5	14.9	R	41	cw	1.6–1.75 Ma (Van Hinsbergen et al., submitted for publication(a))
Mani Peninsula	mean											
MA 1	MA 1–10	10	8	1	342.7	43.4	28.9	10.5	N	17	ccw	4.0–3.8 Ma (Van Hinsbergen et al., submitted for publication(a); Frydas, 1993)
MA 2	MA 11–20	10	8	1	230.5	−17.7	27.0	10.9	R	51	cw	2.0–0.46 Ma (Van Hinsbergen et al., submitted for publication(a))
Messina Peninsula	mean											
MP 1	MP 1–10	10	2	2	190.8	−21.8	–	–	R	11	cw	5.1–4.2 Ma (Van Hinsbergen et al., submitted for publication(a); Frydas, 1993)
MP 2	MP 11–20	10	8	2	164.6	−38.8	10.0	18.4	R	15	ccw	Plio/Pleistocene (Frydas, 1990; Frydas and Bellas, 1994)
MP 3	MP 21–30	10	6	2	160.1	−32.3	19.4	15.6	R	20	ccw	Plio/Pleistocene (Frydas, 1990; Frydas and Bellas, 1994)
MP 4	MP 31–40	10		3	–	–	–	–	–	–	–	1.75–1.6 (Van Hinsbergen et al., submitted for publication(a))
PE 7850[9]			10	1	177.7	−44.3	157.0	3.5	R	2	ccw	Plio/Pleistocene (Laj et al., 1982)

Na=number of analysed samples, Nc=number of conclusive samples, q=quality (1=conclusive, 2=indicative, 3=inconclusive), decl=declination, incl=inclination, *k*=Fisher's precision parameter (Fisher, 1953), α95=95% cone of confidence, pol=polarity, rot=amount of rotation, sense=sense of rotation (cw=clockwise, ccw=counterclockwise).

generally considered to represent a local rotation, caused by, e.g., landsliding [site BO 2, PK4, AA2 and NI3 (Fig. 9; Table 2) and EE4 (Fig. 8; Table 1)]. Only sites PY2 and PY6 both give conclusive results indicating 90° counterclockwise (ccw) or 270°cw rotation. The absence of any structural evidence for such extreme rotations leads us to consider these rotations as either very local, or as a poorly understood artefact. As mentioned above, present-day directions may have overprinted reverse ChRM directions, in particular, because of the overlap in temperature or coercivity spectrum (Fig. 5f). Such sites have been disregarded from our interpretation (e.g., SZ2, SZ3 and SZ6 in Fig. 9 and Table 2). All other sites probably reflect a declination direction that is representative for the entire locality.

4.1. Regional rotations: results from pre-Middle Miocene rocks

To determine the dimension of the domain rotations through time, we compare the new and previously published results obtained from sites and localities in pre-Middle Miocene rocks, as suggested by Kissel and Laj (1988) and Kissel et al. (2003) since these predate the major clockwise rotation of western Greece.

Localities DD and EE cover a large part of the Eocene to Lower Miocene of the Mesohellenic Basin and have declinations of 51±11° and 52±15°, respectively (Figs. 2 and 8; Table 1). The average rotation of all successful sites in the Mesohellenic Basin is 51±8°cw rotation and is interpreted as a basin-wide phenomenon. These findings contradict those of Kissel and Laj (1988) and Márton et al. (1990) who reported rotations of 27±10°cw and 15±26°cw in Oligocene and Miocene rocks, respectively. Our large number of sites and their internal consistency as shown from the successful reversal test (Table 1), however, lead us to believe that ~50°cw rotation is a realistic value.

Following Horner and Freeman (1983), we determined the relationship between the azimuth of the fold axes and the amount of rotation measured from the limbs of the folds in the Lower Oligocene base of the Ionian flysch and the sedimentary sequence of the Mesohellenic Basin. The resulting rotation-corrected strikes are shown in the histogram of Fig. 11, indicating generally E–W trending prerotation strikes. Combination of the rotation data with the azimuth of the major fold axes allows the identification of some zones of local rotation. The general strike of the Ionian and Tripolitza zones and the Mesohellenic

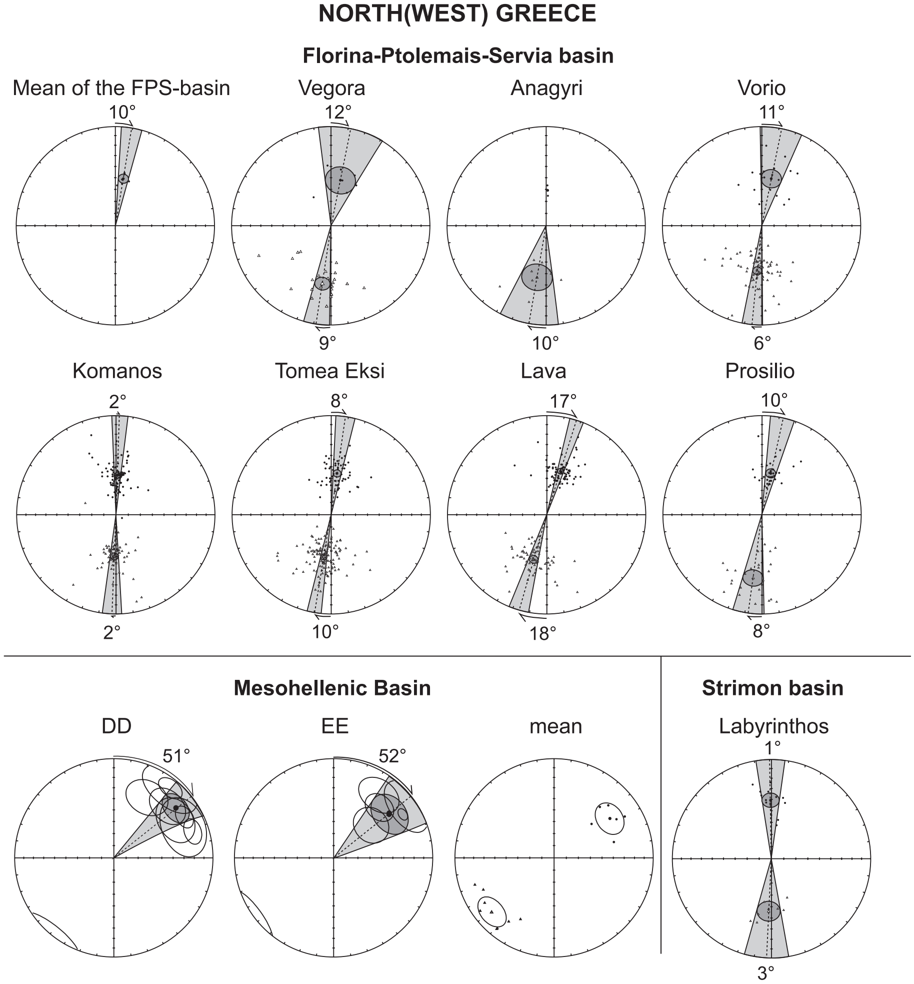

Fig. 8. Results of the NRM analysis for the sites in the Florina–Ptolemais–Servia Basin, the Mesohellenic Basin and the Strymon basin. Closed circles (open triangles) represent normal (reversed) polarities. See Figs. 1 and 2 and Snel et al. (in press) for locations and Table 1 for further details.

Basin at the opposite side of the Pindos Mountains is 330–340°. Localities sampled in anticlines with these strikes in western Greece (KE, SZ, GP, KL, LP, NT, Fig. 3) indicate an average rotation of 49±5°cw. These results are in excellent agreement with the results of Horner and Freeman (1983), who calculated 48±4°cw rotation based on 50 sites in the Paleocene and Eocene Ionian limestones. Three localities in Oligocene flysch of Kissel et al. (1985) give somewhat larger rotations of 55±6°cw, 63,±11°cw and 62° ±19°cw, but still within the error.

The localities of the Lower Miocene in the Botsara-syncline and, of less quality, Kryopigi give rotations of 69±10°cw and 39±20°cw, respectively. Kissel et al. (1985) reported 53±8°cw rotation from the Lower Miocene of the Botsara syncline, which is in better agreement with the net ~50°cw rotation of western Greece.

The 49±5°cw rotation obtained from the Lower Oligocene of the Ionian flysch and the 51±8°cw of the Mesohellenic Basin is comparable to values obtained for 14.8- and 13.2-Ma-old andesites on Evia (51±12°cw) by Morris (1995) and 58±8°cw by Kissel et al. (1989). The 15-Ma-old andesites of the island of Skyros east of Evia and 50- to 30-Ma-old granodiorites on the Chalkidiki peninsula revealed lower values of

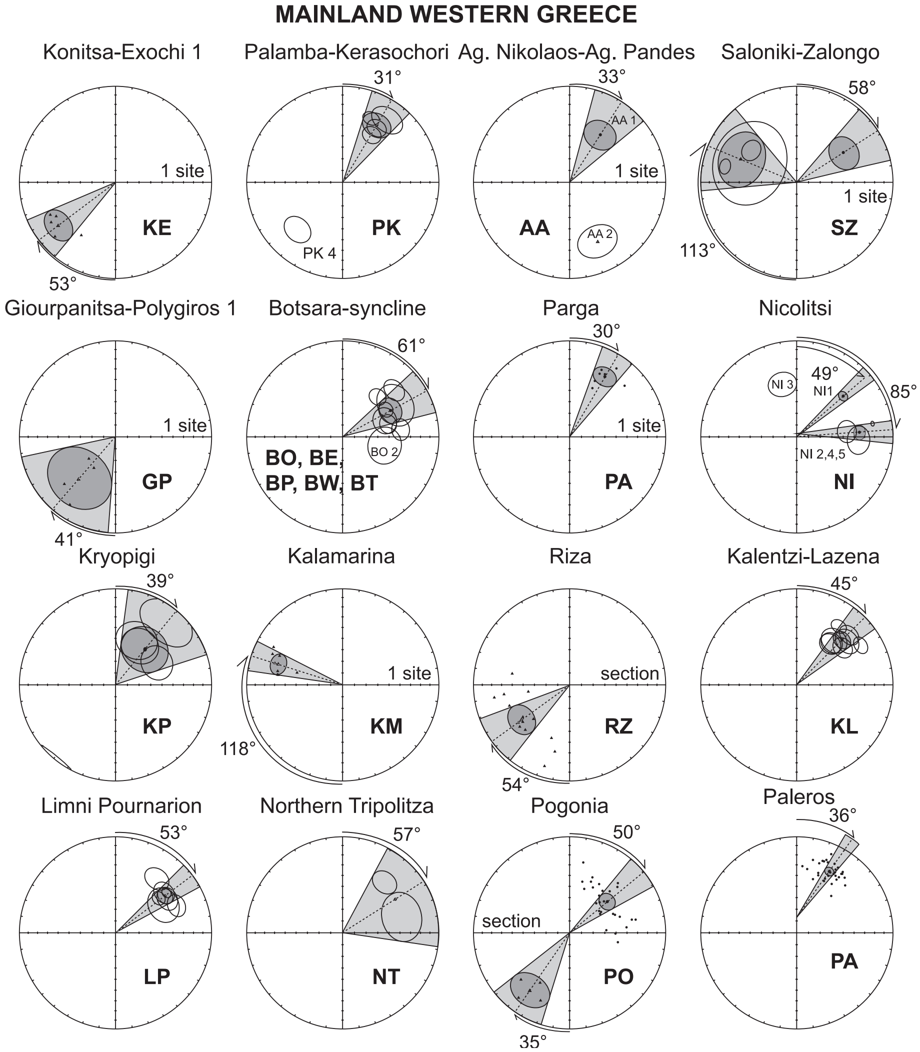

Fig. 9. Results of the NRM analysis for the sites in Epirus and Akarnania, mainland western Greece. Closed circles (open triangles) represent normal (reversed) polarities. See Fig. 3 for locations and Table 2 for further details.

26±8°cw and 37±9°cw rotation, respectively (Kissel et al., 1986a, 1989; Kondopoulou and Westphal, 1986) and from the island of Limnos, Westphal and Kondopoulou (1993) reported 34°±15°cw rotation. These rotations may either indicate that a structure accommodating at least part of the rotation lies between western Greece and Chalkidiki and Skyros. However, especially in the case of Skyros, this is highly uncertain. On the other hand, the rotation of Limnos was explained by Westphal and Kondopoulou (1993) as a result of dextral strike–slip motion along the north-Aegean trough. The islands of eastern Greece (Lesbos, Chios) show no or counterclockwise post-Middle Miocene rotations (Table 4; Kissel et al., 1986a; Kondopoulou et al., 1993a,b).

Smaller clockwise rotations, generally not exceeding 30°cw on the Rhodope, were interpreted as local rotations due to dextral strike–slip motion associated with the North Aegean Trough, without regional significance (Atzemoglou et al., 1994; Dimitriadis et al., 1998; Kondopoulou, 2000).

Speranza et al. (1995) and Mauritsch et al. (1995) reported values of 40–45°cw rotation from pre-Middle Miocene rocks from the external Albanides. It should

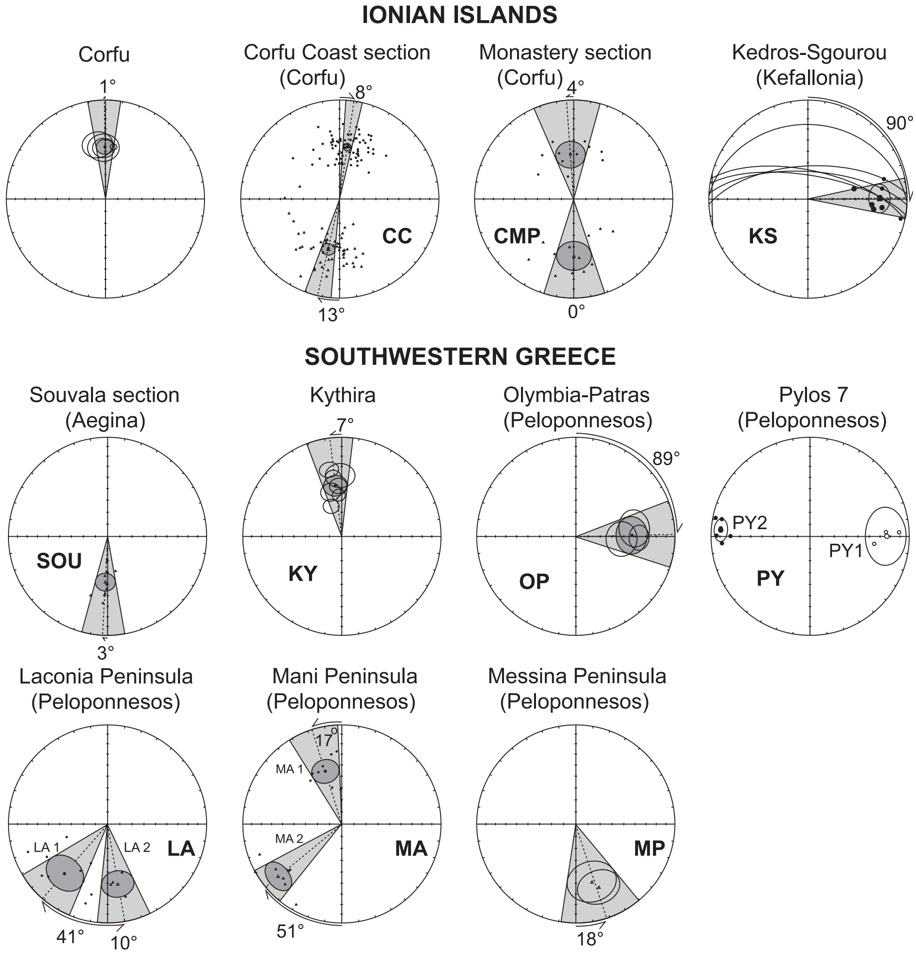

Fig. 10. Results of the NRM analysis for the sites on the Ionian islands (western Greece) and southwestern Greece. Closed circles (open triangles) represent normal (reversed) polarities. See Figs. 3 and 4 for locations and Tables 2 and 3 for further details.

be noted, however, that these values represent rotation with respect to the African reference direction of Besse and Courtillot (1991). Thus, approximately 5–6° should be added to compare them with our results, again yielding rotation values ranging from 45 to 50°cw.

On eastern Peloponnesos, Morris (1995) estimated that approximately 40°cw rotation with respect to the African reference direction occurred after the Late Cretaceous, following a Cretaceous 40–50° rotation phase associated with collision and nappe stacking. We consider our data from locality PY as unreliable and the 96±25°cw rotation of locality OP on the northwestern Peloponneses probably contains an additional local clockwise rotation associated with younger deformation (see below).

Based on the above analysis, we must conclude that the large phase of clockwise rotation that occurred in Greece during the Neogene affected an area covering at least the external Albanides, Epirus and Akarnania, the Mesohellenic Basin and Evia, at least partly the Chalkidiki peninsula and possibly the north Aegean islands Limnos and Skyros and probably also the Peloponnesos. Based on the post-13.2 Ma rotation of Evia (Kissel et al., 1989; Morris, 1995) and the rotation of the Klematia–Paramythia Basin (with an age up to 17 Ma: IGRS-IFP, 1966), the clockwise rotation of the western Aegean occurred

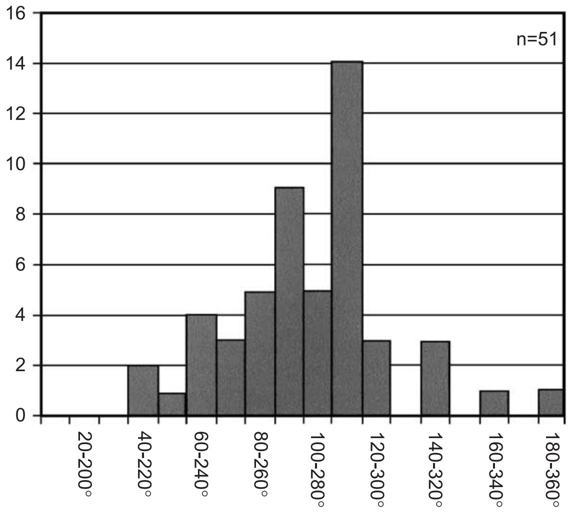

Fig. 11. Frequency diagram of the azimuth of the fold axes at rotation-corrected sites.

after the Early Miocene, as suggested by Kissel and Laj (1988).

4.2. Local rotations: results from pre-Middle Miocene rocks

Some localities in pre-Middle Miocene sediments have significantly different rotation values. These deviations can be straightforwardly explained in terms of local tectonic features.

For example, localities PK and AA near the Albanian border in the northwest of western Greece (Fig. 3) are sampled on the limbs of 310° striking anticlines and give an average rotation value of 31±9°cw. This lower rotation value corresponds to a local relative sinistral bending of approximately 20° in the azimuth of the fold axes. Into Albania, the anticlines reassume a strike of 330–340°. Correction for the local strike change yields approximately 50°cw rotation.

On the limbs of the Thesprotiko anticline, locality NI was sampled, which strikes 340° in the south (corresponding to site NI1, with a 49±4°cw rotation), bending into a 010° strike in the north (where sites NI2, 4 and 5 give 85±6°cw rotation). This bending occurs along the right-lateral Thesprotiko shear zone (Fig. 2). Correction for the 30° of local rotation yields approximately 55°cw rotation. The age of the Thesprotiko antiform postdates the early Miocene based on the tight folding of early Miocene sediments in the Dodoni and Botsara–Kryopigi synclines, which lie east and west of the Thesprotiko anticline and its northern equivalent (Avramidis et al., 2000; IGRS-IFP, 1966). The activity of the Thesprotiko dextral shear zone postdates the folding of the Early Miocene sediments, since it offsets the Botsara syncline. Moreover, the Lower Miocene of Kalamarina and the Lower Pliocene of Riza, which lie on top of the shear zone, rotated 118±8°cw and 54±12°cw, respectively. These anomalously high amounts of rotation fit well with the dextral sense of shear.

Finally, locality OP on the northern Peloponnesos indicates a 96±20°cw rotation and is positioned on 010° striking fold axes. The additional dextral rotation can be explained by its position on the southern side of an eastward plunging antiform that is superimposed on the 340–010° striking tight folds, as can be constructed from the geologic map (Bornovas and Rontogianni-Tsiabaou, 1983; Fig. 4). The antiform disappears towards the west and is therefore a local phenomenon.

In summary, mainland Greece and probably the (northern) Peloponnesos underwent approximately 50° of clockwise rotation, which is in places modified by local rotations, which are well explained by local tectonic phenomena.

4.3. Results from Middle Miocene to Pleistocene rocks

As concluded above, approximately 50°cw rotation affected an area that covers mainland Greece, the external Albanides, Evia and probably the Peloponnesos. The Chalkidiki peninsula and the islands of Skyros and Limnos of northern Greece rotated 30–40°cw. No rotation information is available from time-equivalent (pre-middle Miocene) formations on Crete.

As concluded above, the maximum age for the rotation phase of mainland western Greece, the (external) Albanides and the Peloponnesos is middle Miocene (13.2–14.8 Ma on Evia).

The new sites and sections analysed from younger sediments, together with published information enables to further constrain the timing of the rotation episodes.

The seven sections of the Late Miocene (8 Ma)–Early Pliocene (4 Ma) Florina–Ptolemais–Servia Basin east of the Mesohellenic Basin (Fig. 2) yielded

Table 4
Overview of the published and new rotation data of western and northern Greece, corrected for bedding tilt

Locality	Nc	Decl	Incl	*k*	α95	Pol	Rot	Sense	Age	Reference
Northern and eastern Greece										
Prosilio–Ptelomais–Florina Basin	7	9.7	50.2	241.2	3.9	N/R	10	c	4.0 Ma	(Steenbrink, 2001; Van Vugt et al., 1998; Steenbrink et al., 2000), this study
Ptolemais	1	4.0	50.0	21.0	15.0	N	4	c	1–5 Ma	(Westphal et al., 1991)
Limnos		34.0	48.0	18.0	15.0	N	34	c	17–21 Ma	(Westphal and Kondopoulou, 1993)
Lesbos		6.0	49.0	25.0	7.0	N	6	c	14–15 Ma	(Kissel et al., 1986a)
Chios		155.0	−45.0	18.0	12.0	R	25	cc	15–17 Ma	(Kondopoulou et al., 1993b)
Mesohellenic Basin										
EE and DD sites	14	51.3	23.7	23.3	8.4	N/R	51	c	E. Miocene	this study
SM sites	5	27.0	47.0	16.0	10.0	N/R	27	c	36–24 Ma	(Kissel and Laj, 1988)
Molasse/Limestones		15.0	37.0	23.0	26.0	N/R	15	c	Miocene	(Márton et al., 1990)
Epirus/Akarnania										
Konitsa–Exochi	1	232.9	−26.0	39.6	12.3	R	53	c	Oligocene	this study
Palamba–Kerasochori	4	30.9	31.1	68.9	11.1	N/R	31	c	Oligocene	this study
Aghios Nikolaos–Aghios Pandes	1	32.8	40.9			N	33	c	Oligocene	this study
Saloniki–Zalongo	2	46.1	38.8			N	46	c	E. Oligocene	this study
Botsar syncline	7	61.3	42.6	35.7	10.2	N/R	61	c	E. Miocene	this study
EP sites	14	52.7	−43.6	29.0	7.5	N/R	53	c	Oligocene	(Kissel et al., 1985)
Parga	1	30.4	28.1	46.6	8.9	N/R	30	c	M. Miocene	this study
Nicolitsi	3	85.6	34.3	34.3	21.4		86	c	Oligocene	this study
Kryopigi 1	4	39.6	47.8	51.3	13.0	N	40	c	E. Miocene	this study
Kalamarina	1	287.7	−30.5	51.8	7.8	R	118	c	E. Pliocene	this study
Riza	18	233.9	−37.9	11.9	12.0	R	54	c	Early Pliocene	this study
Kalentzi–Lazena	8	45.4	34.0	58.7	7.3	N	45	c	Oligocene	this study
Ellinikon–syncline	5	54.5	32.1	188.0	5.6	N/R	55	c	Oligocene	(Kissel et al., 1985)
Limni Paroullion	7	53.3	35.7	84.2	6.6	N/R	53	c	Oligocene	this study
Dodoni	5	244.1	−31.1	51.3	10.8	N/R	63	c	Oligocene	(Kissel et al., 1985)
Northern Tripolitza	2	52.3	33.8			N/R	52	c	Oligocene	this study
Epirus	50	48.1	43.6	25.2	4.1	N/R	48	c	Eocene	(Horner and Freeman, 1983)
Paleros	1	35.5	41.1	48.9	3.7	N	36	c	Pliocene	this study
Paleros	1	34.5	49.0	30.0	22.9	N	35	c	Pliocene [this study]	(Birch, 1990)
Pogonia	1	50.3	47.9	17.0	7.0	N	50	c	L. Miocene	this study
Southern Akarnania	5	62.4	30.1	17.9	18.6	N/R	62	c	L. Miocene	(Kissel et al., 1985)
Kerkyra	13	10.8	45.5	31.2	7.5	N/R	11	c	E. Pliocene	(Laj et al., 1982), this study
Corfu Coast*	1	8.9	45.7	24.6	2.6	N/R	9	c	E. Pliocene	(Linssen, 1991), this study
KE 79/80*	9	15.9	44.8	25.5	10.4	N/R	16	c	E. Pliocene	(Laj et al., 1982)
Monastery	1	0.0	46.3	13.6	8.5	N/R	0		E. Pliocene	this study
Lefkimmi 1	1	171.6	−43.7	23.9	11.6	R	8	ac	E. Pliocene	this study
Arillas Beach	1	353.8	43.4	17.9	9.7	N/R	6	ac	Tortonian	this study
Levkas										
Ionian zone	9	90.0	43.0	17.0	13.0	N/R	90	c	Eocene/Oligocene	(Márton et al., 1990)
Pre-apulian zone	13	23.0	32.0	6.0	16.0	N/R	23	c	Eocene/Oligocene	(Márton et al., 1990)
Kephallonia										
Kedros–Sgourou	1	89.5	28.3		10.2	N	90	c	5.08–4.52 Ma	this study
Lixourion (southern Paliki)	1	176.6	−51.2	45.1	2.6	N/R	3	ac	~1.8 Ma	(Duermeijer et al., 2000)
Southern Paliki	1	8.8	53.1	316.3	5.2	N/R	9	c	L. Pliocene	(Laj et al., 1982)
Spartia	1	161.7	−44.0	26.0	5.5	R	18	ac	Plio/Pleistocene	(Duermeijer et al., 2000)
Liakas	1	168.3	−38.2	17.0	10.8	N/R	12	ac	L. Miocene–E. Plioc.	(Duermeijer et al., 2000)

Table 4 (*continued*)

Locality	Nc	Decl	Incl	*k*	α95	Pol	Rot	Sense	Age	Reference
Zakynthos	8	21.6	48.4	128.0	4.9	N/R	22	c	0.77 Ma	(Duermeijer et al., 2000)
Glifa	4	178.0	−59.0	85.0	7.6	R	2	ac	3 Ma	(Kissel et al., 1986b)
Skyros island	4	26.0	45.5	82.0	7.7	N	26	c	15 Ma	(Kissel et al., 1989)
Volos	1	178.0	−59.0	82.0	8.0	R	2	ac	3 Ma	(Kissel et al., 1989)
Evvia										
Kimi Coast	4	199.0	−42.1	62.2	11.7	R	19	c	Miocene	(Morris, 1995)
Oxylithos	4	230.8	−40.3	55.0	12.5	R	51	c	14.8, 13.2 Ma	(Morris, 1995)
EU sites	6	228.3	−43.8	53.0	7.8	R	58	c	15 Ma	(Kissel et al., 1989)
PG 09	1	269.9	−11.5	37.0	6.9	R	90	c	L. Senonian–Maastrichtian	(Morris, 1995)
Attica										
Nea Palatia–Kalamos	1	26.1	51.8	331.0	4.2	N	26	c	L. Mio–Pliocene	(Morris, 1995)
PG 01–04	4	247.8	−41.7	48.9	13.3	N/R	68	c	Oxfordian	(Morris, 1995)
Milos	5	354.8	48.2	30.2	14.2	N/R	5	ac	Plio/Pleistocene	(Duermeijer et al., 2000)
Basalt	1	171.6	−24.2	43.4	9.3	R	8	ac	Pliocene	(Duermeijer et al., 2000)
Myl10	1	11.2	51.2	73.6	9.0	N	11	c	Plio/Pleistocene	(Duermeijer et al., 2000)
Myl11	1	354.4	56.4	359.1	4.0	N	6	ac	Plio/Pleistocene	(Duermeijer et al., 2000)
Myl15	1	348.9	57.1	66.8	7.4	N	11	ac	Plio/Pleistocene	(Duermeijer et al., 2000)
Tsuovala (Hot) (overprinted)	1	–	–	–	–	R	–	–	4.8–3.8 Ma	(Van Hinsbergen et al., 2004)
Volcanics		349.0	50.0	46.0	9.0	N	11	ac	1–3 Ma	(Kondopoulou and Pavlides, 1990)
Aegina	2	180.6	46.9			R	1	c	5.5–<1.6 Ma	(Van Hinsbergen et al., 2004; Morris, 2000); this study
Kythira	6	355.2	47.4	35.8	11.3	N	5	ac	E. Plionece	(Duermeijer et al., 2000); this study
Peloponnesos										
Argolis (Bathonian sites)	7	265.1	−32.2	23.8	12.6	N/R	85	c	Bathonian	(Morris, 1995)
Argolis (DT)	25	220.0	−18.0	103.0	2.9	R	40	c	Senon.–Paleocene	(Morris, 1995)
Tripolis Province	15	40.2	42.9	4.7	19.9	N/R	40	c	Maastrichtian	(Morris, 1995)
Olympia–Patras	3	96.3	32.6	25.3	25.0	N/R	96	c	Oligocene	this study
Isthmus	1	2.7	46.7			N/R	3	c	Plio/Pleistocene	(Duermeijer et al., 2000)
Megara	1	2.7	46.7	35.5	7.4	N/R	3	c	Plio/Pleistocene	(Duermeijer et al., 2000)
Pyrgos Basin	12	10.4	52.0	78.8	4.9	N/R	10	c	Plio/Pleistocene	(Duermeijer et al., 2000)
Corinth Canal	1	177.4	−57.9	26.3	15.2	N/R	3	ac	Pleistocene	(Duermeijer et al., 2000)
Megalopolis	1	1.2	52.6	52.0	2.4	R/N	1	c	0.9–0.25 Ma	(Duermeijer et al., 2000; Van Vugt et al., 2001)
Laconia 1	1	170.4	−38.3	59.3	12.0	N	10	ac	Plio/Pleistocene	this study
Laconia 2	1	221.0	−34.1	11.5	14.9	R	41	c	1.6–1.75 Ma	this study
Evrotas Basin	5	16.6	48.6	117.3	7.1	N/R	17	c	Plio/Pleistocene	(Duermeijer et al., 2000; Laj et al., 1982)

Nc=number of conclusive samples, decl=declination, incl=inclination, *k*=Fisher's precision parameter (Fisher, 1953), α95=95% cone of confidence, pol=polarity, rot=amount of rotation, sense=sense of rotation (cw=clockwise, ccw=counterclockwise).

a very consistent set of rotations, on average 10±4°cw. The reversal test (McFadden and McElhinny, 1990) was successful for most sections. This suggests that the last 10±4°cw of the total of 50°cw rotation occurred after 4 Ma and no rotations occurred between 8 and 4 Ma. The Early Pliocene site Klimataki (KH) in the Mesohellenic Basin (Fountoulis et al., 2001) is inconclusive, as is the 4±15°cw rotation obtained for the Ptolemais area by Westphal et al. (1991).

In Epirus, the Middle Miocene sediments near Parga, lying below a ~290° striking SSW verging thrust, rotated 30°cw. This could mean that approximately 20°cw rotation occurred prior to the deposition of the Parga marls. Taking the azimuth of the fold axes and the strike of the thrusts near Parga into account, it is more likely that local relative counterclockwise rotation occurred as was suggested for localities PK and AA (Figs. 3 and 9; Table 2).

The Upper Miocene (Tortonian) sediments of the Arillas Beach section on Corfu give results with high uncertainties. The sections and sites in the Pliocene of Corfu, however, show rotations varying from 8±12°ccw to 9±3°cw (Fig. 9, Table 2). It should be noted that most sections give 'type 2' measurements with large uncertainties. Our new values are lower than those reported previously from Corfu (16±10°cw; Laj et al., 1982). Combination of our results with those of Laj et al. (1982) yields a rotation of 11±8°cw for Corfu since the Pliocene. This value is comparable with the post-4 Ma 10±4°cw rotation obtained from the Florina–Ptolemais–Servia basin.

The Tortonian sections Pogonia, Paleros and the Pliocene sections of Riza along the western coast of Epirus, as well as Kedros–Sgourou on Kefallonia (Fig. 3), show large clockwise rotations. The rotation of section Riza has above been explained by its position on top of, or close to, the right-lateral Thesprotiko shear zone (Fig. 3). Sections Pogonia and Paleros, opposite to Levkas, experienced a young, post-Tortonian rotation of 50±7°cw and 36±4°cw, respectively. The sections lie on the eastern, partly overturned limb of an east-verging anticline. The tight folding is probably the result of transpression along the Kefallonia Fault Zone, as was proposed for 010°-striking, E-verging folds in the north of the nearby island of Levkas by Cushing (1985). This interpretation is confirmed by the 90±13°cw rotation of N–S striking antiforms in the Ionian zone of southeast Levkas reported by Márton et al. (1990). At present, the strike of the Pogonia section is 020° and the strike of the Paleros section is 360°. Subtracting the post-Tortonian 50±7°cw and 36±4°cw rotations from these strikes yields a pre-Tortonian strike of 330–340°, i.e., parallel to the general present-day trend of the Hellenides. Thus, we suggest that the post-Tortonian rotation of the Pogonia and Paleros sections is a local phenomenon induced by drag folding along the Kefallonia Fault Zone, superimposed on the major 50° rotation of western Greece.

The Lower Pliocene of the Kedros–Sgourou section on the north of the 010–020° striking Paliki peninsula of west Kefallonia gives an ill-defined rotation of 90±10°cw. It should be noted that this rotation is mainly based on two oriented hand specimens. The large rotation value, however, could be very well explained by drag folding along the Kefallonia Fault Zone, especially since there is a difference in azimuth of the folds on the main island of Kefallonia with those on the Paliki peninsula of approximately 70°. At the south coast of the Paliki peninsula, rotations varying from 3±3°ccw (Duermeijer et al., 2000) to 9±5°cw (Laj et al., 1982) were reported. Activity of a southeast-verging young normal fault on southern Kefallonia probably explains the counterclockwise rotations in the order of 15±5°ccw (Duermeijer et al., 2000) measured in the Plio-Pleistocene sections in its hangingwall . The large rotation obtained for the Kedros–Sgourou section and, further north, for the Riza, Pogonia and Paleros sections occurred probably mainly in the course of the Pliocene and is attributed to the effect of drag folding along the dextral Kefallonia Fault Zone offshore and the equally dextral Thesprotiko shear zone on land.

In summary, the rotations of the late Neogene sections that were sampled on Kefallonia and in Epirus can all best be explained as local rotations. They therefore do not further constrain the timing of the rotation phases of the western Aegean.

A 20–25°cw rotation phase of the island of Zakynthos (Fig. 1) and the ~17°cw rotation of the Evrotas Basin on the southeastern Peloponneses (Fig. 4) led Laj et al. (1982), Kissel and Laj (1988), Duermeijer et al. (1999, 2000) and Kissel et al. (2003) to conclude that the ~50°cw rotation of western Greece occurred in two episodes of 25°: one before the Late Miocene and one during the Plio-Pleistocene (Kissel and Laj, 1988; Laj et al., 1982). The rotation of Zakynthos was later redated as post-770 kyr by Duermeijer et al. (1999). Results obtained from the peri-Adriatic depression in northern Albania, where tightly folded Pliocene marls have been reported to rotate by 23±9°cw (Speranza et al., 1995), provided additional evidence for this interpretation and led Speranza et al. (1995) to conclude that the Vlore–Elbesan–Diber transverse zone and the Kefallonia Fault Zone, which lie between Zakynthos and the

Peloponnesos in the south and the Peri–Adriatic depression in the north, do not have a significant influence on the rotation of the Hellenides and Albanides.

The data of Duermeijer et al. (2000), however, do not show any significant rotations on the Isthmus of Corinth in the northeast, and the Megalopolis Basin in the centre of the Peloponnesos since the Plio-Pleistocene and 900 kyr, respectively. The Pyrgos Basin on the northwestern Peloponnesos shows a rotation of only 10±5°cw since the Late Pliocene (recalculated from the results of Duermeijer et al., 2000) and the southern peninsulas of the Peloponnesos give a variety of rotations in opposite directions (Figs. 4 and 10; Table 3). The island of Kythira, located south of the southeastern peninsula of the Peloponnesos gives evidence for small counterclockwise rotation (Figs. 4 and 10; Table 3), noticed earlier by Duermeijer et al. (2000). The island of Aegina in the Saronic Gulf does not show any rotation since the Late Miocene (Pontian; Figs. 4 and 10; Table 3), as was also concluded by Morris (2000).

The varying amounts and senses of Plio-Pleistocene rotations suggest that most of these rotations—including the Pleistocene 20–25°cw rotation of Zakynthos (Duermeijer et al., 1999; Laj et al., 1982)—are the result of local tectonic phenomena and do not reflect regional rotation. All rotation results have been obtained in and immediately adjacent to faults that have been highly active since the Late Pliocene, such as the Sparta and Kalamata faults, the Gulf of Patras–Gulf of Corinth fault system, the Sperchios–Gulf of Evia fault system and the Kefallonia Fault Zone (Armijo et al., 1991, 1996; Koukouvelas et al., 1996; Koukouvelas and Doutsos, 1996; Kranis and Papanikolaou, 2001; Lyon-Caen et al., 1988; Mariolakos et al., 1989; Ori, 1989; Roberts and Jackson, 1991; Sorel, 2000; Stavrakakis, 1996; Westaway, 2002). The regional Pliocene rotation phase of 25° suggested by Laj et al. (1982), Kissel and Laj (1988), Speranza et al. (1995) and Kissel et al. (2003) for western Greece and Albania is in our view mainly based on these local rotations and should therefore be reconsidered.

The area in which the Late Pliocene extensional basins, with their internal local rotations developed appears to be bound in the north by the Kefallonia Fault Zone and the Amvrakikos–Sperchios–Evia half-graben system and the North Anatolian Fault Zone/North Aegean Trough system. Reliable information on the timing of the large rotation phase should be obtained from outside the area deformed by these fault zones.

The two localities in Greece that meet this criterion are Corfu and the Florina–Ptolemais–Servia Basin, which are located on the western and eastern parts of the rotating domain, respectively. Both localities appear to have undergone a post-Pliocene rotation of approximately 10° and no rotation between 8 and 4 Ma. Therefore, the majority of the rotation (~40°cw) of the western Aegean seemingly occurred between approximately 13–15 and 8 Ma, and only 10°cw occurred since approximately 4 Ma. This is in good agreement with the orientations of stretching lineations of Walcott and White (1998), who also concluded a post-Early Pliocene 10° rotation of the west-Aegean domain.

The Late Miocene (Messinian) Labyrinthos section in the Strimon basin does not reveal any significant rotation (1±7°cw, Table 1, Fig. 1), which might indicate that the Pliocene rotation did not include the Strimon basin, although it should be noted that this suggestion is based on only one section.

Speranza et al. (1995) argued that the 25°cw rotation of the Peri-Adriatic depression in northern Albania represents a regional rather than a local clockwise rotation, based on the comparable amount of rotation found on Zakynthos. Following the same line of reasoning, we suggest that the Pliocene clockwise rotation measured in the Peri-Adriatic depression probably did have a component of local rotation., which may have been associated with the phase of tight folding that affected the area.

5. On the dimension of the rotating domain and the structures accommodating the rotations of the western Aegean

The above analysis shows that an area from northern Albania to probably the south Peloponnesos and from Corfu to Evia underwent a clockwise rotation of ~50° between the Middle Miocene (probably 13 Ma) and the early Late Miocene (8 Ma). Further east, an area covering the Chalkidiki peninsula and possibly also the islands of Skyros and Leros was affected by approximately 30–40°cw rotation (Fig. 12). It cannot be concluded from the presented data that the western Aegean rotated as a rigid body, but if deformation—

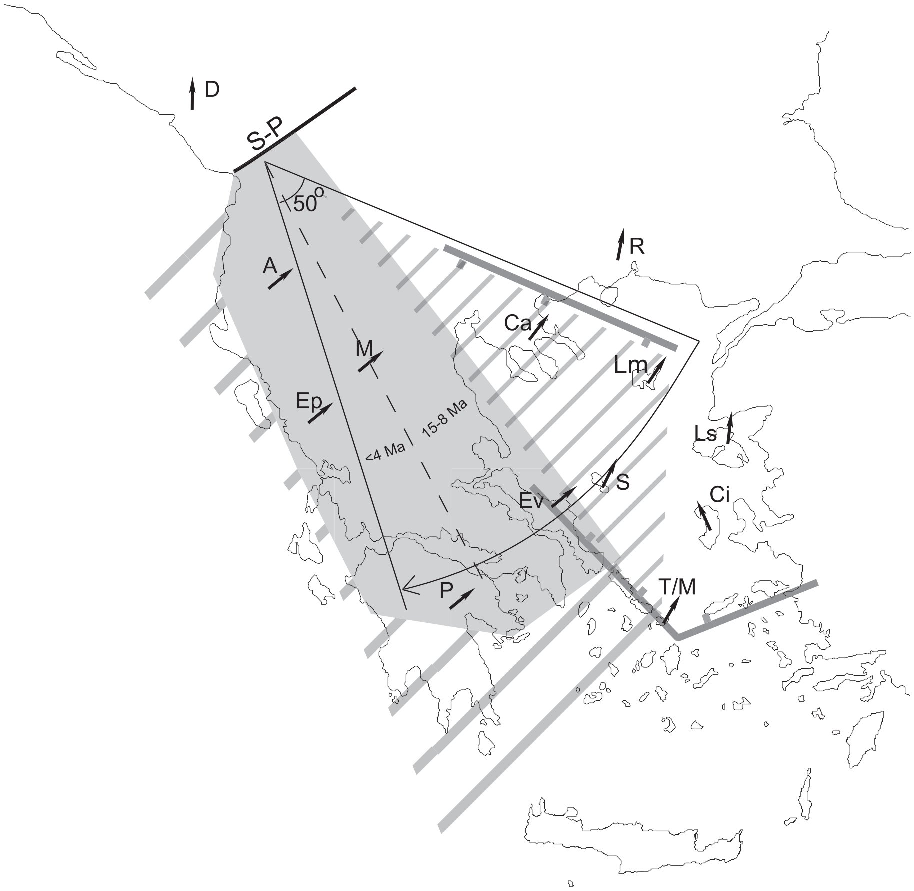

Fig. 12. Schematic map indicating the configuration of the domain that rotated clockwise in the western Aegean region since the middle Miocene. The shaded area is inferred to rotate 50°cw. The finely hatched area has smaller finite post-Oligocene clockwise rotations of 30–40°. The widely hatched area does not contain middle Miocene sediments but it is inferred from structural observations that it belonged to the 50°cw rotating domain. A=Albanides; Ca=Chalkidiki peninsula; Ci=Chios; D=Dinarides; Ep=Epirus; Ev=Evia; Lm=Limnos; Ls=Lesbos; M=Mesohellenic basin; P=Peloponnesos; R=Rhodope; S=Skyros; S–P=Scutari–Pec transform; T/M=Tinos and Mykonos.

compressional or extensional—occurred, it did not lead to significant internal rotations.

This rotating domain underwent internal deformation leading to loci or zones with a deviating total amount of rotation. This section summarises the most probable candidates for the accommodation of the motion associated with the rigidly rotating western Aegean domain since the Middle Miocene. The northern limit of the Aegean rotations has been identified by Kissel et al. (1995), who concluded that the Scutari–Pec fault zone in northern Albania is the best candidate to form the transition zone from no significant post-Eocene rotations in the Dinarides to a 50°cw rotation of the Albano–Hellenides. The Scutari–Pec fault zone is a complex zone along which in the Tertiary right-lateral transpression occurred (Meco and Aliaj, 2000) and which was interpreted by Robertson and Shallo (2000) to represent a Mesozoic transform fault. The northern limit of the rotating domain is not studied in detail in this paper, but the fact that no large-scale extension occurred along the eastern part of the Scutari–Pec fault zone indicates that at least the northern part of the rotating domain did not behave entirely as a rigid body. The northern boundary of the rotating domain was not studied in detail in this paper.

To identify the western limit, the results of studies that have been carried out to reconstruct the rotation history of the Apulian platform in Italy and Greece are reviewed. Scheepers (1992) showed that the Apulian peninsula of southeastern Italy did not undergo any Pleistocene rotation. Tozzi et al. (1988) found ~25° post-Eo-Oligocene clockwise rotation along the southeastern coast of the Apulian peninsula, whereas Speranza and Kissel (1993) found no post-Eo-Oligocene rotation on the Gargano peninsula further north. It should be noted, however, that both Tozzi et al. (1988) and Speranza and Kissel (1993) indicate that they cannot exclude a remagnetisation of their samples. Therefore, these results are ambiguous. Further west in the Calabrian arc, counterclockwise rotations prevail since the Tortonian (Duermeijer et al., 1998b).

Duermeijer et al. (1999) stated that no pre-Pleistocene, post-Early Miocene rotation occurred of the pre-Apulian zone of Zakynthos. Márton et al. (1990) found approximately 90° of rotation of the pre-Apulian zone of Levkas, which can best be explained as the result of drag folding along the Kefallonia Fault Zone. In conclusion, the Apulian platform did not rotate probably, and if it did, not more than 25°cw rotation occurred. Therefore, the present boundary between the Ionian zone and (Pre-) Apulian zone, i.e., the Ionian thrust, served to accommodate (a large part of) the rotational motion.

The age of the Ionian thrust has previously been dated around 4 Ma (Mercier et al., 1972, 1976; Underhill, 1989). Because nappe emplacement is not likely to be an instantaneous event, this age estimate probably marks the end of activity. As was noticed by Speranza et al. (1995), approximately 350 km of horizontal motion probably took place during rotation at the latitude of the Gulf of Corinth. The Ionian thrust must have accommodated the majority of this shortening. South of the Apulian platform, the Hellenic subduction zone probably bounded the rotating domain, as it was present throughout the Tertiary (Spakman et al., 1993).

From the southern Aegean islands, no data are available from sediments older than approximately 10 Ma. Duermeijer et al. (1998a, 2000) reported post-Early Messinian 0° to 50°ccw rotation on Crete, Rhodos, Karpathos and Kythira (Fig. 1). Combination with fault kinematic analysis led Duermeijer et al. (1998a) to ascribe these counterclockwise rotations to sinistral strike–slip faults, associated with the Pliny and Strabo trench fault system. Further north on the Cyclades, 30°ccw rotation was found in granodiorites from Naxos (Morris and Anderson, 1996), whereas 20–30°cw rotation was reported from 11-Ma-old intrusives from Mykonos and Tinos by Avigad et al. (1998) and Morris and Anderson (1996). These granodiorites entered the brittle field around 10 Ma (Gautier and Brun, 1994). As the magnetisation of the granodiorites was mainly carried by pyrrhotite with an unblocking temperature of ~320°C (Morris and Anderson, 1996), which is a temperature typical for the brittle–ductile transition, 10 Ma can be considered as the maximum age of the rotation. Counterclockwise rotations (5±14°ccw) were also reported from Milos (Duermeijer et al., 2000; Kondopoulou and Pavlides, 1990).

These rotation data combined with the orientations of stretching lineations throughout the Cyclades led Walcott and White (1998) to construct a discrete lineament (Mid-Cycladic lineament) as the boundary of the western Aegean rotating domain. The eastern border of the rotating domain, according to Walcott and White (1998) and later Kondopoulou (2000), is ill-defined and located in the northern Aegean and the northern Rhodope. During the rotation phase, extension in the Aegean domain was accommodated among others by the extensional detachments of the Cyclades and the Rhodope (Fig. 1), as can be inferred from the geochronological and fission track data obtained from Miocene granites (e.g., Altherr et al., 1982; Hejl et al., 2002; Lips et al., 2000). Therefore, probably at least part of the rotation difference between, for instance, the Chalkidiki peninsula and the Rhodope, and between the Cycladic islands of Tinos and Mykonos and Chios can be explained by the activity of these detachments. The role of the detachments in the rotation history of Greece will be the subject of future work.

6. Summary and conclusions

The combination of new and previously published paleomagnetic data allows us to draw the following conclusions:

(1) The clockwise rotation of the western Aegean domain occurs on a region between northern Albania and (at least the northern part of) the Peloponnesos and western Greece and Evia. An area covering the Chalkidiki peninsula and possibly the islands of Limnos and Skyros did

rotate clockwise, but with a smaller finite rotation of 30–40°.

(2) The large data set and the detailed geologic information make it possible to distinguish local rotations from the regional ones.

(3) The regional clockwise rotation of western Greece takes place in two episodes: 40°cw between ~15–13 and 8 Ma and an additional 10°cw rotation after 4 Ma ago.

(4) The area affected by Late Plio-Pleistocene deformation is dominated by strike–slip related rotations: counterclockwise rotations on Crete are associated with the activity of the left-lateral Pliny and Strabo Trenches and clockwise rotations on the Ionian islands and western Akarnania are associated with the activity of the right-lateral Kefallonia Fault Zone. A dispersed pattern of rotations is found in between on the southern Peloponnesos.

(5) The rotations are accommodated by deformation associated with the Scutari–Pec fault zone in the north and the Ionian thrust and the Hellenic subduction zone in the west. In the south, no rotation information was obtained from rocks older than 9.8 Ma. From existing data, it follows that Crete did not rotate as a rigid body after this time.

(6) The early rotation phase of western Greece occurred contemporaneously with motion along the extensional detachment systems of the Cyclades and the Rhodope. This extension accommodates probably at least part of the differential rotation between northern and eastern Greece and the western rotating domain.

(7) Aegean extension, initiated between 20 and 30 Ma, did not involve rotation until <15 Ma.

Acknowledgements

Anthony Morris and an anonymous reviewer are acknowledged for their useful comments on the manuscript. Pavlos Avramidis (Sedimentological laboratory, University of Patras, Greece) is kindly thanked for the excursion days in the Klematia–Paramythia and Mesohellenic basins and the stimulating discussions. Rinus Wortel is acknowledged for critical reading of earlier versions of the manuscript. Paul Meijer is thanked for fruitful discussion. Laurent Jolivet kindly provided his papers-in-press. Mark-Jan Sier, Douwe van der Meer, Suzanne Bijl, Yiannis Dimitriou, Iannis Vakalas, Georgios Ananiadis and Aris Mantzios are thanked for their help during the sampling campaigns and the stimulating field discussions. Marianne Leewis analysed the samples of the Mesohellenic Basin and the Botsara sections. Erik Snel, Joris Steenbrink and Nicole van Vugt kindly provided their paleomagnetic data on the Strimon and Florina–Ptolemais–Servia and Basins.

References

Altherr, R., et al., 1982. A late Oligocene/Early Miocene high temperature belt in the Attica Cycladic crystalline complex (SE Pelagonian, Greece). Geol. Jahrb., Reihe E Geophys. 23, 97–164.

Angelier, J., 1981. Analyse quantitative des relations entre déformation horizontale et mouvements verticaux: l'extension égéenne, la subsidence de la mer de Crète et la surrection de l'arc hellénique. Ann. Géophys. 37 (2), 327–345.

Armijo, R., Lyon-Caen, H., Papanastassiou, D., 1991. A possible normal-fault rupture for the 464 BC Sparta earthquake. Nature 351, 137–139.

Armijo, R., Meijer, B., King, G.C.P., Rigo, A., Papanastassiou, D., 1996. Quarternary evolution of the Corinth Rift and its implications for the Late Cenozoic evolution of the Aegean. Geophys. J. Int. 126, 11–53.

Armour-Brown, A., De Bruijn, H., Maniati, C., Siatos, G., Niesen, P., 1979. The geology of the Neogene sediments north of Serrai and the use of rodent faunas for biostratigraphic control. Proceedings of the VI Colloquium on the Geology of the Aegean Region, vol. 2, pp. 612–622.

Atzemoglou, A., Kondopoulou, D., Papamarinopoulos, S., Dimitriadis, S., 1994. Paleomagnetic evidence for block rotations in the Western Greek Rhodope. Geophys. J. Int. 118 (1), 221–230.

Avigad, D., Baer, G., Heimann, A., 1998. Block rotations and continental extension in the central Aegean Sea: palaeomagnetic and structural evidence from Tinos and Mykonos (Cyclades, Greece). Earth Planet. Sci. Lett. 157, 23–40.

Avramidis, P., Zelilidis, A., 2001. The nature of deep-marine sedimentation and palaeocurrent trends as evidence of Pindos foreland basin fill conditions. Episodes 24 (4), 252–256.

Avramidis, P., Zelilidis, A., Kontopoulos, N., 2000. Thrust dissection control of deep-water clastic dispersal patterns in the Klematia–Paramythia foreland basin, western Greece. Geol. Mag. 137 (6), 667–685.

Avramidis, P., Zelilidis, A., Vakalas, I., Kontopoulos, N., 2002. Interactions between tectonic activity and eustatic sea-level changes in the Pindos and Mesohellenic basins, NW Greece. J. Pet. Geol. 25 (1), 53–82.

Barbieri, R., 1992a. Foraminifera of the Eptachorion formation (early Oligocene) of the Mesohellenic Basin, northern Greece. J. Micropaleontol. 11, 73–84.
Barbieri, R., 1992b. Oligocene through Palaeogene/Neogene boundary foraminifera of the northern Mesohellenic Basin (Macedonia, Greece): biostratigraphy and palaeoecologic implications. Palaeogeogr. Palaeoclimatol. Palaeoecol. 99, 193–211.
Benda, L., Van der Meulen, A.J., Meyer, K.-J., Van de Weerd, A., 1987. Biostratigraphic correlations in the Eastern Mediterranean Neogene: 8. Calibration of sporomorph- and rodent-associations from the Megalopolis Basin (Peloponnesus, Greece). Newsl. Stratigr. 17 (3), 129–141.
Besse, J., Courtillot, V., 1991. Revised and synthetic apparent polar wander parths of the African, Eurasian, North-American and Indian plates, and true polar wander since 200 Ma. J. Geophys. Res. 96 (B3), 4029–4050.
Billiris, H., et al., 1991. Geodetic determination of tectonic deformation in central Greece from 1900 to 1988. Nature 350, 124–129.
Birch, W.G., 1990. Paleomagnetic studies in western and central Greece: tectonic evolution of the Aegean domain since the Triassic, unpub. theses, Liverpool University. 321 pp.
Bizon, G., et al., 1983. Données nouvelles sur le Néogène et le Quarternaire des escarpements ioniens (Méditerranée orientale). Rev. Inst. Fr. Pét. 38 (5), 575–603.
Bonneau, M., 1984. Correllation of the Hellenic Nappes in the south-east Aegean and their tectonic reconstruction. In: Dixon, J.E., Robertson, A.H.F. (Eds.), The Geological Evolution of the Eastern Mediterranean. Geological Society of London, London, pp. 517–527.
Bornovas, I., Rontogianni-Tsiabaou, T., 1983. Geological Map of Greece. Institute of Geological and Mineral Exploration, Athens.
B.P. Co. Ltd., 1971. The geological results of petroleum exploration in Western Greece, Athens.
Caputo, R., Pavlides, S., 1993. Late Cainozoic geodynamical evolution of Thessaly and surroundings (central–northern Greece). Tectonophysics 223, 339–362.
Clews, J.E., 1989. Structural controls on basin evolution: Neogene to Quarternary of the Ionian zone, Western Greece. J. Geol. Soc. (Lond.) 146 (3), 447–457.
Cocard, M., et al., 1999. New constraints on the rapid crustal motion of the Aegean region: recent results inferred from GPS-measurements (1993–1998) across the West Hellenic Arc, Greece. Earth Planet. Sci. Lett. 172, 39–47.
Cushing, E.M., 1985. Evolution struturale de la marge nord ouest Hellénique dans l'ile de Levkas et ses environs (Grece nord-occidentale), unpub. Thesis, Universite de Paris-Sud. Centre d'orsay, Paris. 295 pp.
Dimitriadis, S., Kondopoulou, D., Atzemoglou, A., 1998. Dextral rotations and tectonomagmatic evolution of the southern Rhodope and adjacent regions (Greece). Tectonophysics 299, 159–173.
Dinter, D.A., 1998. Late Cenozoic extension of the Alpine collisional orogen, Northeastern Greece: origin of the north Aegean basin. Geology 21, 45–48.
Dinter, D., Royden, L., 1993. Late Cenozoic extension in north-eastern Greece: Strymon Valley detachment system and Rhodope metamorphic core comples. Geol. Soc. Amer. Bull. 90, 84–92.
Doutsos, T., Kontopoulos, N., Poulimenos, G., 1988. The Corinth–Patras rift as the initial stage of continental fragmentation behind an active island arc (Greece). Basin Res. 1, 177–190.
Doutsos, T., Kontopoulos, N., Poulimenos, G., Frydas, F., Piper, D.J.W., 1990. Geologic history of the extensional basin of the Gulf of Corinth (?Miocene–Pleistocene), Greece—Comment. Geology 18, 1256.
Doutsos, T., Koukouvelas, I., Zelilidis, A., Kontopoulos, N., 1994. Intracontinental wedging and post-orogenic collapse in the Mesohellenic Trough. Geol. Rundsch. 83, 257–275.
Duermeijer, C.E., Krijgsman, W., Langereis, C.G., Ten Veen, J.H., 1998. Post early Messinian counter-clockwise rotations on Crete: implications for the late Miocene to recent kinematics of the southern Hellenic Arc. Tectonophysics 298 (1–3), 77–89.
Duermeijer, C.E., Van Vugt, N., Langereis, C.G., Meulenkamp, J.E., Zachariasse, W.J., 1998b. A major late Tortonian rotation phase in the Crotone basin using AMS as tectonic tilt correction and timing of the opening of the Tyrrhenian basin. Tectonophysics 287, 233–249.
Duermeijer, C.E., et al., 1999. A Late Pleistocene clockwise rotation phase of Zakynthos (Greece) and implications for the evolution of the western Aegean arc. Earth Planet. Sci. Lett. 173, 315–331.
Duermeijer, C.E., Nyst, M., Meijer, P.T., Langereis, C.G., Spakman, W., 2000. Neogene evolution of the Aegean arc: paleomagnetic and geodetic evidence for a rapid and young rotation phase. Earth Planet. Sci. Lett. 176, 509–525.
Fisher, R.A., 1953. Dispersion on a sphere. Proc. R. Soc. Lond., A 217, 295–305.
Fountoulis, I., et al., 2001. The presence of marine Pliocene sediments in the Mesohellenic Trough (Pramoritsa banks, Grevena, Greece). Bull. Geol. Soc. Greece 19 (2), 603–612.
Frydas, D., 1990. Plankton-Stratigraphie des Pliozäns und unteren Pleistozäns der SW-Peloponnes, Griechenland. Newsl. Stratigr. 23 (2), 91–108.
Frydas, D., 1993. Über die Nannoplankton-Stratigraphie des Pliozäns des SE-Peloponnes, Griechenland. Neues Jahrb. Geol. Paläontol., Monatsh. 4, 227–238.
Frydas, D., Bellas, S., 1994. Plankton stratigraphy and some remarks on Globorotalia evolutionary trends from the Plio-Pleistocene of southwestern Peloponnesus, Greece. Micropaleontology 40 (4), 322–336.
Gautier, P., Brun, J.-P., 1994. Ductile crust exhumation and extensional detachments in the central Aegean (Cyclades and Evvia Islands). Geodin. Acta 7, 57–85.
Gautier, P., et al., 1999. Timing, kinematics and cause of Aegean extension: a scenario based on a comparison with simple analogue experiments. Tectonophysics 315, 31–72.
Hageman, J., 1977. Stratigraphy and sedimentary history of the Upper Cenozoic of the Pyrgos-area (Western-Peloponnesus), Greece. Ann. Géol. Pays Hell. 1977, 298–333.
Hejl, E., Riedl, H., Weingartner, H., 2002. Post-plutonic unroofing and morphogenesis of the Attic–Cycladic complex (Aegea, Greece). Tectonophysics 349, 37–56.

Horner, F., Freeman, R., 1983. Palaeomagnetic evidence from Pelagic Limestones for clockwise rotation of the Ionian zone, Western Greece. Tectonophysics 98, 11–27.

IGRS-IFP, 1966. Étude Géologique de l'Épire (Grèce nord-occidentale). Editions Technip, Paris. 306 pp.

Jolivet, L., Patriat, M., 1999. Ductile extension and the formation of the Aegean Sea. In: Durand, B., Jolivet, L., Horvath, F., Séranne, M. (Eds.), The Mediterranean Basins: Tertiary extension within the Alpine Orogen, Spec. Publ.-Geol. Soc. Lond. London, pp. 427–456.

Jolivet, L., et al., 1996. Miocene detachment on Crete and exhumation P–T–t paths of high-pressure metamorphic rocks. Tectonics 15 (6), 1129–1153.

Jolivet, L., Facenna, C., Goffé, B., Burov, E., Agard, P., 2003. Subduction tectonics and exhumation of high-pressure metamorphic rocks in the Mediterranean orogen. Am. J. Sci. 303, 353–409.

Jolivet, L., Rimmelé, G., Oberhänsli, R., Goffé, B., Candan, O., 2004. Correlation of syn-orogenic tectonic and metamorphic events in the Cyclades, the Lycian Nappes and the Menderes Massif. Geodynamic implications. Bull. Soc. Géol. Fr. (in press).

Jordan, G., et al., submitted for publication. A GIS framework for digital tectonic geomorphology, with case studies in Hungary and NW Greece. Int. J. Appl. Earth Observ. Geoinform.

Kahle, H.-G., et al., 1998. The strain rate field in the eastern Mediterranean region estimated by repeated GPS measurements. Tectonophysics 294, 237–252.

Kissel, C., Laj, C., 1988. The tertiary geodynamical evolution of the Aegean arc: a paleomagnetic reconstruction. Tectonophysics 146, 183–201.

Kissel, C., Laj, C., Müller, C., 1985. Tertiary geodynamical evolution of northwestern Greece: paleomagnetic results. Earth Planet. Sci. Lett. 72, 190–204.

Kissel, C., Laj, C., Mazaud, A., 1986a. Paleomagnetic results from Neogene formations in Evia, Skyros and the Volos region and the deformation of Central Aegea. Geophys. Res. Lett. 13, 1446–1449.

Kissel, C., et al., 1986b. Paleomagnetic evidence for Neogene rotational deformations in the Aegean domain. Tectonics 5 (5), 783–796.

Kissel, C., Laj, C., Poisson, A., Simeakis, K., 1989. A pattern of block rotations in central Aegea. In: Kissel, C., Laj, C. (Eds.), Paleomagnetic Rotations and Continental Deformation. Kluwer Academic Publishers, pp. 115–129.

Kissel, C., Speranza, F., Milicevic, V., 1995. Paleomagnetism of external southern Dinarides and northern Albanides: implications for the Cenozoic activity of the Scutari–Pec shear zone. J. Geophys. Res. 100 (B8), 14999–15007.

Kissel, C., Laj, C., Poisson, A., Görür, N., 2003. Paleomagnetic reconstruction of the Cenozoic evolution of the Eastern Mediterranean. Tectonophysics 362, 199–217.

Kondopoulou, D., 2000. Paleomagnetism in Greece: Cenozoic and Mesozoic components and their geodynamic implications. Tectonophysics 326, 131–151.

Kondopoulou, D., Pavlides, S., 1990. Paleomagnetic and neotectonic evidence for different deformation patterns in the South Aegean volcanic arc: the case of Milos island. Proceedings of the IESCA, Izmir, vol. 1, pp. 210–223.

Kondopoulou, D., Westphal, M., 1986. Paleomagnetism of the tertiary intrusive from Chalkidiki (northern Greece). J. Geophys. 59, 62–66.

Kondopoulou, D., De Bonis, L., Koufos, G., Sen, S., 1993a. Paleomagnetic data and biostratigraphy of the Middle Miocene vertebrate locality of Thymiana, Chios island, Greece. Proceedings of the 2nd Congress of the Hellenic Geophysical Union, Florina, pp. 676–687.

Kondopoulou, D., Leci, V., Symeakis, C., 1993b. Paleomagnetic study of the Tertiary volcanics in Chios Island, Greece. Proceedings of the 2nd Congress of the Hellenic Geophysical Union, Florina, pp. 676–687.

Kontopoulos, N., Fokianou, T., Zelilidis, A., Alexiadis, C., Rigakis, N., 1999. Hydrocarbon potential of the middle-Eocene–middle Miocene Mesohellenic piggy-back basin (central Greece): a case study. Mar. Pet. Geol. 16, 811–824.

Koukouvelas, I.K., Doutsos, T.T., 1996. Implications of structural segmentation during earthquakes: the 1995 Egion earthquake, Gulf of Corinth, Greece. J. Struct. Geol. 18 (12), 1381–1388.

Koukouvelas, I., Mpresiakas, A., Sokos, E., Doutsos, T., 1996. The tectonic setting and earthquake ground hazards of the 1993 Pyrgos earthquake, Peloponnese, Greece. J. Geol. Soc. (Lond.) 153, 39–49.

Kranis, H.D., Papanikolaou, D.I., 2001. Evidence for detachment faulting on the NE Parnassos mountain front (Central Greece). Bull. Geol. Soc. Greece 34 (1), 281–287.

Laj, C., Jamet, M., Sorel, D., Valente, J.P., 1982. First paleomagnetic results from Mio-Pliocene series of the Hellenic Sedimentary arc. Tectonophysics 86, 45–67.

Le Pichon, X., Angelier, J., 1979. The Hellenic arc and trench system: a key to the neotectonic evolution of the Eastern Mediterranean area. Tectonophysics 60, 1–42.

Linssen, J.H., 1991. Properties of Pliocene sedimentary geomagnetic reversal records from the Mediterranean. Geol. Ultraiectina 80, 1–231.

Lips, A.L.W., White, S.H., Wijbrans, J.R., 2000. Middle–Late Alpine thermotectonic evolution of the southern Rhodope Massif, Greece. Geodin. Acta 13, 281–292.

Lyon-Caen, H., et al., 1988. The 1986 Kalamata (South Peloponnesus) Earthquake: detailed study of a normal fault, evidences for East–West extension in the Hellenic Arc. J. Geophys. Res. 93 (B12), 14,967–15,000.

Mariolakos, I., 1976. Thoughts and view points on certain problems of the geology and tectonics of the Peloponnesus (Greece). Ann. Géol. Pays Hell. 27, 215–313.

Mariolakos, I., Fountoulis, I., Logos, E., Lozios, S., 1989. Surface faulting caused by the Kalamata (Greece) earthquakes (13.9.86). Tectonophysics 163, 197–203.

Márton, E., Papanikolaou, D.J., Lekkas, E., 1990. Paleomagnetic results from the Pindos, Paxos and Ionian zones of Greece. Phys. Earth Planet. Inter. 62 (1–2), 60–69.

Mauritsch, H.J., Scholger, R., Bushati, S.L., Ramiz, H., 1995. Palaeomagnetic results from southern Albania and their

significance for the geodynamic evolution of the Dinarides, Albanides and Hellenides. Tectonophysics 242, 5–18.
McFadden, P.L., 1990. A new fold-test for palaeomagnetic studies. Geophys. J. Int. 103, 163–169.
McFadden, P.L., McElhinny, M.W., 1988. The combined analysis of remagnetisation circles and direct observations in paleomagnetism. Earth Planet. Sci. Lett. 87, 161–172.
McFadden, P.C., McElhinny, M.W., 1990. Classification of the reversal test in palaeomagnetism. Geophys. J. Int. 103, 725–729.
McKenzie, D., 1978. Active tectonics of the Alpine–Himalayan belt: the Aegean Sea and surrounding regions. Geophys. J. R. Astron. Soc. 55, 217–254.
Meco, S., Aliaj, S., 2000. Geology of Albania. Beitraege zur regionalen Geologie der Erde vol. 28. Gebrueder Borntraeger, Berlin. 246 pp.
Mercier, J., et al., 1972. Déformations en compression dans le Quarternaire des rivages ioniens (Céphalonie, Grèce). Données néotectoniques et séismiques. C. R. Acad. Sci. Paris 275, 2307–2310.
Mercier, J.-L., Carey, É., Philip, H. and Sorel, D., 1976. La néotectonique plio-quarternaire de l'arc égéen externe er de la mer Égée er ses relations avec la séismicité. Bull. Soc. Géol. Fr., (7) 18(2): 355–372.
Meulenkamp, J.E., 1979. The Aegean and the Messinian salinity crisis. Proc. of the VI Coll on the Geology of the Aegean Region, vol. 3, pp. 1253–1263.
Meulenkamp, J.E., Theodoropoulos, P., Tsapralis, V., 1977. Remarks on the Neogene of Kythira, Greece. Sixth Coll. Geol. Aegean Region, vol. 1, pp. 355–362.
Meulenkamp, J.E., Wortel, M.J.R., Van Wamel, W.A., Spakman, W., Hoogerduyn Strating, E., 1988. On the Hellenic subduction zone and the geodynamical evolution of Crete since the late Middle Miocene. Tectonophysics 146, 203–215.
Morris, A., 1995. Rotational deformation during Palaeogene thrusting and basin closure in eastern central Greece: palaeomagnetic evidence from Mesozoic carbonates. Geophys. J. Int. 121, 827–847.
Morris, A., 2000. Magnetic fabric and paleomagnetic analyses of the Plio–Quarternary calc-alkaline series of Aegina Island, South Aegean volcanic arc, Greece. Earth Planet. Sci. Lett. 176, 91–105.
Morris, A., Anderson, M., 1996. First palaeomagnetic results from the Cycladic Massif, Greece, and their implications for Miocene extension directions and tectonic models in the Aegean. Earth Planet. Sci. Lett. 142, 397–408.
Ori, G.G., 1989. Geologic history of the extensional basin of the Gulf of Corinth (?Miocene–Pleistocene), Greece. Geology 17, 918–921.
Pavlides, S.B., Mountrakis, D.M., 1987. Extensional tectonics of northwestern Macedonia, Greece, since the late Miocene. J. Struct. Geol. 9 (4), 385–392.
Pavlides, S., Sokoutis, D., Tsaltabasi, A., 1998. The Servia–Kozani Graben Formation; insights from analogue modelling. Bull. Geol. Soc. Greece 32 (1), 137–144.
Peeters, F.J.C., et al., 1998. Differentiating glacio-eustacy and tectonics; a case study involving dinoflagellate cysts from the Eocene–Oligocene transition of the Pindos Foreland Basin (NW Greece). Terra Nova 10, 245–249.
Peter, Y., et al., 1998. Establishment of a continuous GPS network across the Kephalonia Fault Zone, Ionian islands, Greece. Tectonophysics 294, 253–260.
Piper, D.J., Panagos, A.G., Kontopoulos, N., Pe, G.G., 1976. Deposition environments of Pliocene littoral sediments, Gythion, Southern Peloponnese, Greece. Z. Dtsch. Geol. Ges. 127, 435–444.
Piper, D.J.W., Pe-Piper, G., Kontopoulos, N., Panagos, A.G., 1982. Plio-Pleistocene sedimentation in the western Lakonia graben, Greece. Neues Jahrb. Geol. Paläontol., Monatsh. 11, 679–691.
Ricou, L.-E., Burg, J.-P., Godfriaux, I., Ivanov, Z., 1998. Rhodope and Vardar: the metamorphic and the olistostromic paired belts related to the Cretaceous subduction under Europe. Geodin. Acta 11 (6), 285–309.
Roberts, S., Jackson, J., 1991. Active normal faulting in central Greece: an overview. In: Roberts, A.M., Yielding, G., Freeman, B. (Eds.), The Geometry of Normal Faults, Spec. Publ.-Geol. Soc. Lond., pp. 125–142. London.
Robertson, A., Shallo, M., 2000. Mesozoic–Tertiary tectonic evolution of Albania in its regional Eastern Mediterranean context. Tectonophysics 316, 197–254.
Rögl, F., Bernor, R.L., Dermitzakis, M.D., Müller, C., Stancheva, M., 1991. On the Pontian correlation in the Aegean (Aegina Island). Newsl. Stratigr. 24 (3), 137–158.
Scheepers, P., 1992. No tectonic rotation for the Apulia–Gargano foreland in the Pleistocene. Geophys. Res. Lett. 19 (22), 2275–2278.
Snel, E., Marunteanu, M. and Meulenkamp, J.E., in press. Calcareous nannofossil biostratigraphy and magnetostratigraphy of the Upper Miocene and Lower Pliocene of the Northern Aegean (Orphanic Gulf–Strimon Basin areas (Greece). In: J. Agustí and O. Oms (Editors), Palaeogeogr. Palaeoclimatol. Palaeoecol. spec. issue: Late Miocene to Early Pliocene environments and ecosystems in Eurasia.
Sorel, D., 2000. A Pleistocene and still-active detachment fault and the origin of the Corinth-Patras rift, Greece. Geology 28 (1), 83–86.
Sorel, D., Nesteroff, W.D., Limond, J., Lemeille, F., Sebrier, M., 1976. Mise en évidence de structures compressives sous-marines plio–pléistocènes dans l'arc égéen externe au large du Levkas (îles Ioniennes, Grèce). C. R. Acad. Sci. Paris 282, 2045–2048.
Spakman, W., Van der Lee, S., Van der Hilst, R., 1993. Travel-time tomography of the European–Mediterranean mantle down to 1400 km. Phys. Earth Planet. Inter. 79, 3–74.
Speranza, F., Kissel, C., 1993. First paleomagnetism of Eocene rocks from Gargano: widespread overprint or non-rotation? Geophys. Res. Lett. 20 (23), 2627–2630.
Speranza, F., Islami, I., Kissel, C., Hyseni, A., 1995. Palaeomagnetic evidence for Cenozoic clockwise rotation of the external Albanides. Earth Planet. Sci. Lett. 129, 121–134.
Stavrakakis, G.N., 1996. Strong motion records and anthetic isoseismals of the Pyrgos, Peloponnisos, Southern Greece, earthquake sequence of March 26, 1993. Pure Appl. Geophys. 146 (1), 147–161.

Steenbrink, J., 2001. Orbital signatures in lacustrine sediments: the late Neogene intramontane Florina–Ptolemais–Servia Basin, northwestern Greece. Geol. Ultraiectina 205, 167.

Steenbrink, J., Van Vugt, N., Hilgen, F.J., Wijbrans, J.R., Meulenkamp, J.E., 1999. Sedimentary cycles and volcanic ash beds in the Lower Pliocene lacustrine successions of Ptolemais (NW Greece): discrepancy between $^{40}Ar/^{39}Ar$ and astronomical ages. Palaeogeogr. Palaeoclimatol. Palaeoecol. 152, 283–303.

Steenbrink, J., van Vugt, N., Kloosterboer-van Hoeve, M.L., Hilgen, F.J., 2000. Refinement of the Messinian APTS from sedimentary cycles patterns in the lacustrine Lava section (Servia Basin, NW Greece). Earth Planet. Sci. Lett. 181, 161–173.

Steffens, P., De Bruijn, H., Meulenkamp, J.E., Benda, L., 1979. Field guide to the Neogene of Northern Greece (Thessaloniki area and Strimon basin). Publ. Dep. Geol. Paleontol. Univ. Athens, Ser. A 35, 1–14.

Tauxe, L., Watson, G.S., 1994. The fold test: an eigen analysis approach. Earth Planet. Sci. Lett. 122, 331–341.

Theye, T., Seidel, E., 1991. Petrology of low-grade high-pressure metapelites from the External Hellenides (Crete, Peloponnese.). A case study with attention to sodic minerals. Eur. J. Mineral. 3, 343–366.

Tozzi, M., Kissel, C., Funiciello, R., Laj, C., Parotto, M., 1988. A clockwise rotation of southern Apulia? Geophys. Res. Lett. 15 (7), 681–684.

Underhill, J.R., 1988. Triassic evaporites and Plio–Quarternary diapirism in western Greece. J. Geol. Soc. (Lond.) 145, 269–282.

Underhill, J.R., 1989. Late Cenozoic deformation of the Hellenide foreland, western Greece. Geol. Soc. Amer. Bull. 101, 613–634.

Van Hinsbergen, D.J.J., et al., 2004. Vertical motions in the Aegean volcanic arc: evidence for rapid subsidence preceding in situ volcanism. Mar. Geol. 209, 329–345.

Van Hinsbergen, D.J.J., Van der Meer, D.G., Meulenkamp, J.E., submitted for publication(a). Internal deformation of western Greece during Neogene clockwise rotation and collision with Apulia. submitted to Int. J. Earth Sci.

Van Hinsbergen, D.J.J., Zachariasse, W.J., Wortel, M.J.R., Meulenkamp, J.E., submitted for publication(b). Underthrusting and exhumation: A comparison between the External Hellenides, the 'hot' Cycladic and 'cold' South Aegean core complexes. submitted to Tectonics.

Van Vugt, N., 2000. Orbital forcing in late Neogene lacustrine basins from the Mediterranean. Geologica, 189.

Van Vugt, N., Steenbrink, J., Langereis, C.G., Hilgen, F.J., Meulenkamp, J.E., 1998. Magnetostratigraphy-based astronomical tuning of the early Pliocene lacustrine sediments of Ptolemais (NW Greece) and bed-to-bed correlation with the marine record. Earth Planet. Sci. Lett. 164, 535–551.

Van Vugt, N., Langereis, C.G., Hilgen, F.J., 2001. Orbital forcing in Pliocene–Pleistocene Mediterranean lacustrine deposits: dominant expression of eccentricity versus precession. Palaeogeogr. Palaeoclimatol. Palaeoecol. 172, 193–205.

Walcott, C.R., White, S.H., 1998. Constraints on the kinematics of post-orogenic extension imposed by stretching lineations in the Aegean area. Tectonophysics 298 (1–3), 155–175.

Westaway, R., 2002. The Quarternary evolution of the Gulf of Corinth, central Greece: coupling between surface processes and flow in the lower continental crust. Tectonophysics 348, 269–318.

Westphal, M., Kondopoulou, D., 1993. Paleomagnetism of Miocene volcanics from Lemnos island: implications for block rotations in the vicinity of the north Aegean Trough. Ann. Tecton. 7 (2), 142–149.

Westphal, M., Kondopoulou, D., Edel, J., Pavlides, S., 1991. Paleomagnetism of Tertiary and Plio-Pleistocene formations from N. Greece. Bull. Geol. Soc. Greece 25, 239–250.

Wilpshaar, M., 1995. Applicability of dinoflagellate cyst stratigraphy to the analysis of passive and active tectonic settings. Geologica, 134.

Zelilidis, A., Doutsos, T., 1992. An interference pattern of neotectonic faults in the southwestern part of the Hellenic forearc basin, Greece. Z. Dtsch. Geol. Ges. 143, 95–105.

Zelilidis, A., Kontopoulos, N., 1997. Depositional environments of the Pentapholos formation in the Mesohellenic basin: application to the concept of hydrocarban habitat. Min. Wealth 102, 45–52.

Zelilidis, A., Koukouvelas, I., Doutsos, T., 1988. Neogene paleostress changes behind the forearc fold belt in the Patraikos Gulf area, western Greece. Neues Jahrb. Geol. Paläontol., Monatsh. 1988 (5), 511–525.

Zelilidis, A., Kontopoulos, N., Avramidis, P., Bouzos, D., 1997. Late Eocene to Early Miocene depositional environments of the Mesohellenic Basin, North-Central Greece: implications for hydrocarbon potential. Geol. Balc. 27 (1–2), 45–55.

Zelilidis, A., Piper, D.J.W., Kontopoulos, N., 2002. Sedimentation and basin evolution of the Oligocene–Miocene Mesohellenic basin, Greece. AAPG Bull. 86 (1), 161–182.

Zijderveld, J.D.A., 1967. A.c. demagnetisation of rocks: analysis of results. In: Collinson, D.W., et al., (Eds.), Methods in Palaeomagnetism. Elsevier, Amsterdam, pp. 254–286.

Zygojannis, N., Müller, C., 1982. Nannoplankton-Biostratigrafie der tertiären Mesohellennischen Molasse (Nordwest-Griechenland). Z. Dtsch. Geol. Ges. 133, 442–455.